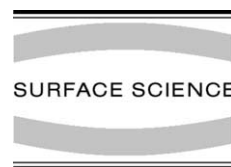




ELSEVIER

Surface Science 500 (2002) 759–792



www.elsevier.com/locate/susc

# The surfaces of compact systems: from nuclei to stars

R.A. Broglia<sup>a,b,\*</sup>

<sup>a</sup> *Department of Physics, University of Milan, and INFN Sez. di Milano, Via Celoria 16, 20133 Milan, Italy*

<sup>b</sup> *The Niels Bohr Institute, University of Copenhagen, Blegdamsvej 17, DK-2100 Copenhagen, Denmark*

Received 30 June 2000; accepted for publication 14 May 2001

---

## Abstract

While providing information from worlds separated by five-to-six orders of magnitude in dimensions and in energy, the pairing properties (electrical resistance and viscosity), the electromagnetic response (spectrum of colours), the resilience to stress (elasticity), the ability to deform (plasticity), etc., associated with clusters of atoms and with atomic nuclei have surprisingly similar properties, once the proper scalings are done, and demonstrate the many analogies that can be drawn between different finite many-body systems. These analogies can be further extended to cosmic and to customer tailored nanometre materials. Femtometre materials, like the inner crust of a neutron star (pulsar), are made out of the same protons and neutrons which make infinite nuclear matter. However in pulsars, protons and neutrons are arranged in the form of finite nuclei immersed in a sea of free neutrons. This is the reason why these celestial objects rotate, conduct heat, emit neutrinos, etc., very differently from infinite nuclear matter. In fact, these phenomena reflect the properties of the corresponding atomic nuclei which form the pulsar. Among these properties, those associated with the nuclear surface are most important. Nanostructured materials are made out of atoms as their more common forms, but the atoms are arranged in nanometre or sub-nanometre-size clusters, which become the constituent grains, or building blocks, of new materials like, e.g., C<sub>60</sub> fullerene. Because these tiny grains respond to light, mechanical stress and electricity quite differently from micron- or millimetre-sized grains, nanostructured materials display an array of novel attributes. At the basis of the new phenomena we find again the surface of the building blocks used to produce the new materials. A proper understanding of the interweaving of the single-particle motion with the static and dynamic deformations of the surface of finite many-body systems is likely to provide the key to open a whole new world of interdisciplinary research in such disparate fields as isolated atomic nuclei and clusters, new materials and compact stellar objects. The concepts and the experimental evidence needed to tool this key will be reviewed. Special emphasis will be set on the open questions still remaining to be answered to reach this goal. © 2001 Elsevier Science B.V. All rights reserved.

**Keywords:** Many body and quasi-particle theories; Superconductivity

---

## 1. Introduction

Finite many-particle systems can be viewed as drops of a liquid of interacting particles (protons and neutrons in the case of atomic nuclei, electrons and ions in the case of atomic aggregates, etc.) held

---

\* Address: Dipartimento di Fisica, Istituto Nazionale di Fisica Nucleare (INFN), University of Milan, Via Celoria 16, 20133 Milan, Italy. Tel.: +39-02-583-57231; fax: +39-02-583-57487.

E-mail address: broglia@mi.infn.it (R.A. Broglia).

together by an elastic surface. To fully understand these systems is quite a formidable task, as already the three-body problem does not allow for an exact solution. Mean field theory is, in most cases, a very useful approximation to the problem. In it, one replaces the many-body equation describing the motion of all particles simultaneously, by the single-particle equation describing the motion of one particle at a time. Consequently particles move independently, in an average potential, which is generated by the particles themselves. The surface of this potential plays a paramount role not only in confining the motion of the particles but also in controlling their spill out. It can also act as an elastic membrane which can vibrate.

The vibrations of the surface of finite many-body systems dress the single-particle motion, renormalizing its properties and consequently, the properties of the entire system. In fact, in their trajectories particles bounce, most of the time, elastically off the surface. From time to time, however, they set the surface into vibration, vibration which can be reabsorbed at a later time by the same particle or by another particle. In the first case the particle carries around a vibration and becomes effectively heavier, which thus modifies, among other things, the specific heat of the system. In the second case, the vibration becomes a messenger between two particles, and thus acts as a glue. The resulting interaction is particularly efficient in producing pairs of particles. These pairs of particles have properties that are very different from those of single particles. In particular they may behave collectively as a liquid without viscosity, or, if charged, without resistance. That is, as a superfluid or as a superconductor.

The vibrational frequencies of the surface of finite many-body systems can be very low, becoming eventually zero in the case in which the surface acquires a permanent, static deformation. Both the single-particle motion and the collective surface vibrations of a deformed system can be quite different from the corresponding properties associated with neighbouring spherical systems.

In the universal language of field theory, first developed in connection with quantum electrodynamics, i.e., the theory describing the interaction of charged particles among themselves and with

photons, these phenomena are associated with self-energy and vertex corrections and with induced interaction processes. These processes are intimately connected among themselves through very general relations, known as sum rules and reflecting the conservation of mass and charge. Furthermore, deformations and zero frequency vibrations are intimately connected with spontaneous symmetry breaking phenomena, and thus with the violation of the conservation of angular momentum, linear momentum, particle number, etc.

In what follows, we shall discuss some of the consequences the coupling of single-particle motion to static and dynamic deformations of the surface has on the physical properties of finite many-body systems. Special emphasis will be placed on the open questions and on the possible practical applications the subject has on the middle ground of physics [1]. The middle ground is an enormous domain, including everything intermediate in size between an atomic nucleus and a stellar object. It is the domain of everyday human experience. We shall start from the very small, the atomic nucleus, a paradigm of finite many-body systems whose properties are dominated by surface effects. This is because nuclei have a large ratio of surface to volume and, being very compact objects, a high surface tension. We shall provide experimental evidence and theoretical insight concerning the workings of the particle–vibration coupling mechanism in atomic nuclei. Pair formation and the phenomenon of superfluidity will be discussed in particular detail, also in connection with newly produced exotic forms of (nuclear) matter not previously observed in the Universe. Utilizing atomic nuclei as building blocks, we shall then concentrate our attention on very large systems, in particular on stellar compact objects. We shall again discuss the phenomenon of pair formation and of superfluidity in these systems, and its connection with the nuclear surface.

Armed with this experimental and theoretical insight we shall then proceed by analogy into the corresponding pair formation phenomenon and pairing in systems belonging to the middle ground of physics. Particular attention will be paid to

superconductivity in nanometre organic materials made out of  $C_{60}$  fullerenes. The strength with which pairs of particles are held together in finite many-body systems due to the exchange of surface vibrations scales with surface tension. While this quantity is many orders of magnitude weaker in fullerenes than in atomic nuclei, the study of pairing in  $C_{60}$  is still a subject of particular interest. In fact, we shall emphasize that there is, potentially, a huge pay off in achieving a detailed understanding of these phenomena. Namely, the possibility of designing a real high  $T_c$  superconductor, that is a material which conducts electricity without resistance at temperatures not too different from room temperature.

After having studied, at the microscopic level, the consequences surface vibrations have on the interaction among particles and resulting in pair formation, we shall see how they affect the colour of finite many-body systems. We shall start the subject by discussing examples that have been around for centuries, namely that of small metallic clusters which give the colours to (stained) glasses. Making use of what one has learned during the last two decades on the “colour” of atomic nuclei, that is the response of nuclei to photons, it will be shown that it is likely that one already has the tools to design materials displaying costume tailored colours. Among other possibilities one can, by properly tuning the shape of the clusters, make them display more or less “metallic colours”. From this knowledge it turns out that one can also design atomic wires which are of potential interest in microelectronics. This is again an open and quite promising subject of research.

We shall conclude the paper by emphasizing the very general physical concepts which explain why the surface of finite many-body systems is so important in determining their properties. Such concepts also explain why it is possible to work out an unified description of a great variety of objects ranging from the atomic nucleus to compact stellar objects, as well as materials which affect our daily life. The same concepts are, not surprisingly, also at the basis of the universal mathematical language used in this description: namely field theory of finite many-body systems.

## 2. Specific heat, superfluidity and superconductivity

The atom is the smallest unit into which matter can be divided that has the characteristic properties of a chemical element. Most of the atom is empty space. The rest consists of a cloud of negatively charged electrons whirling around a small, very dense, positively charged nucleus made out of protons and neutrons and contains essentially all the mass of the atom. The electric forces bind the electrons to the nucleus giving rise to a miniature planetary-like system. The strong and Coulomb forces acting among nucleons lead to a self-bound system. Inside it, nucleons move essentially independently of each other. Bouncing in their trajectories elastically off the nuclear surface, they describe closed orbits which resemble, at a length scale five orders of magnitude smaller, those of the electrons in the atom. This discovery won in 1963 the Nobel prize in physics to Maria Goeppert-Mayer and J. Hans D. Jensen [2].

### 2.1. The atomic nucleus

Nucleons, like electrons are fermions, i.e. have a half-integer spin ( $1/2, 3/2, \dots$ ), and, according to quantum mechanics, obey the Pauli exclusion principle which allows only one particle to occupy each quantal state. Consequently, for the ground state of the system, the available orbitals of the mean field are filled from the bottom upwards to the Fermi energy. Under normal conditions, atomic nuclei are in their ground state, that is at zero temperature. This is because nuclei on earth, leaving aside those that arrive in the form of cosmic rays, are isolated. In fact, for two nuclei to interact, they need to have large kinetic energies, of the order of tens of MeV ( $1 \text{ MeV} = 10^6 \text{ eV}$ ), so as to be able in a collision to overcome the Coulomb repulsion and reach within the range of the nuclear attraction. Energies of such magnitude contrast with the energies available at room temperature ( $\approx 25 \times 10^{-3} \text{ eV}$ ). This is the reason why one needs large machines, so called atomic smashers, to make two atomic nuclei interact. In these machines, an atom containing a heavy atomic nucleus is stripped of most of its electrons becoming a heavy ion, which is subsequently

accelerated and collimated. The resulting beam, aimed at a target of other heavy atomic nuclei, eventually lead to a heavy ion reaction (Fig. 1). In the event where the two nuclei fuse, the energy and angular momentum of relative motion becomes mostly excitation energy and angular momentum of the composite system. Typical values of these quantities are set, in (Fig. 2), in relation to temperatures and rotational frequencies observed in other physical systems. The thermalization of such a system depends, naturally, on the specific heat of the system, a quantity which is directly related to

the density of levels around the Fermi energy and thus to the nuclear surface, as we shall explain in the next section.

### 2.1.1. Single-particle motion

To study the single-particle motion in nuclei the best probe one can use are transfer reactions. For example, aiming a beam of deuterons (the isotope  ${}^2_1\text{H}_1 (\equiv d)$  of hydrogen containing one proton and one neutron) on a target nucleus, one can learn about the properties of the single-particle neutron levels lying above the Fermi energy, by studying

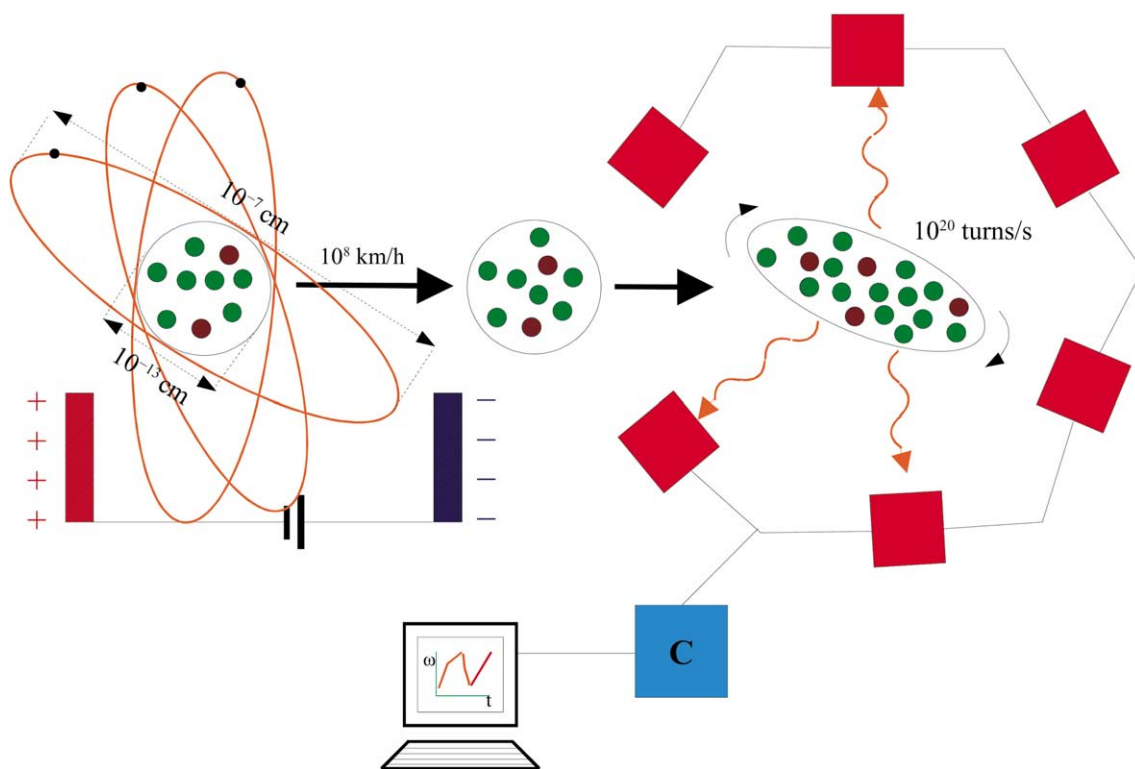


Fig. 1. Schematic representation of a heavy ion accelerator used to induce nuclear reactions. A neutral atom (left part of the figure), formed of a nucleus made out of protons (red dots) and neutrons (green dots), is stripped of the electrons (small black dots) moving around it. The system becomes positively charged and the resulting heavy ion is accelerated to velocities of the order of 100 millions of kilometers per hour in an electric field and smashed against the atomic nuclei of a target (middle). Out of the violent encounter between the two atomic nuclei a number of processes can take place: Coulomb excitation, particle transfer, etc. In some cases the two nuclei fuse, leading to a highly excited, rapidly rotating compound nucleus (right) which, in the process of cooling down, emits nucleons, alpha particles and  $\gamma$ -rays (orange wavy arrows). These  $\gamma$ -rays (photons) can be detected by use of a so called  $4\pi$ -array, that is a set of detectors (red squares) covering a consistent fraction of the solid angle, an example of which is EUROBALL, the powerful array constructed by an European collaboration of nuclear physicists [3]. Once the signal is collected, it is analysed making use of specifically developed computer programs (software labeled C inside blue square) and the results eventually displayed on a screen.

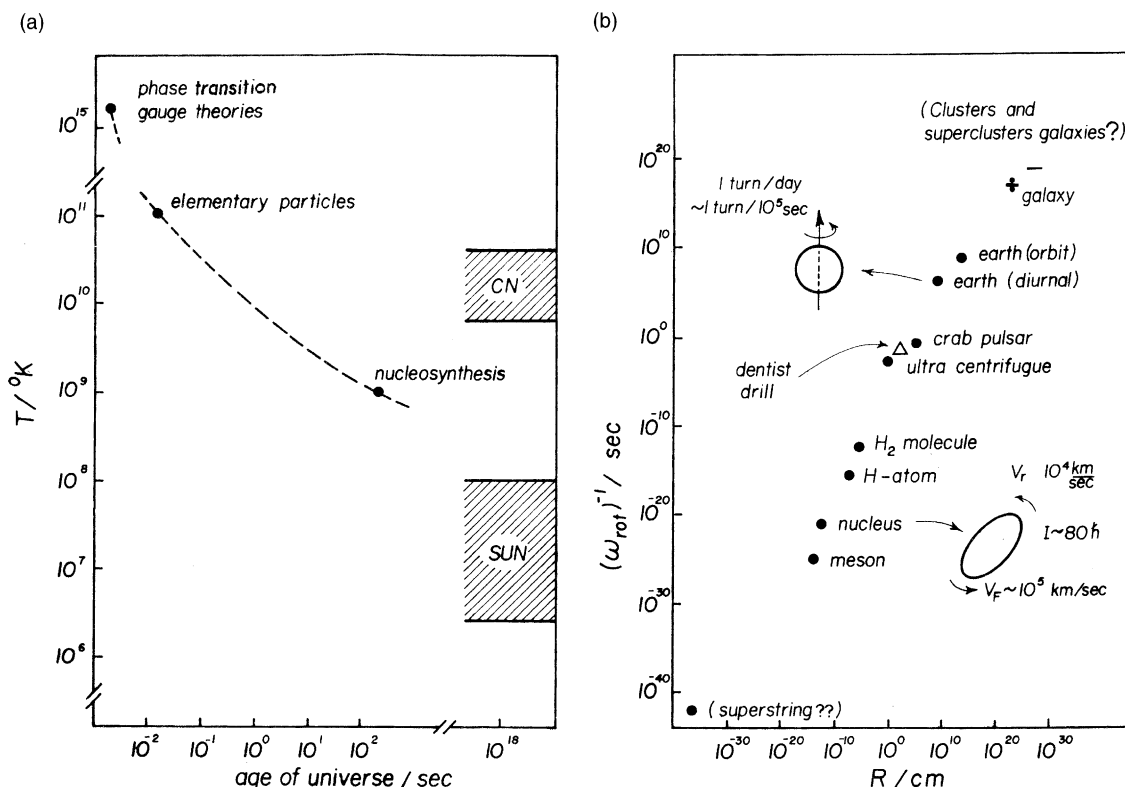


Fig. 2. Temperatures and rotational frequencies typical of reactions where two heavy ions fuse and eventually, after a time of the order of a few times  $10^{-21}$  s equilibrate all their degrees of freedom, forming a single compound nucleus. (a) The scale of temperature has been set in connection with the temperature ascribed to the Universe at different times after the Big Bang through the first 3 min to our times [4]. (b) The inverse of the rotational period (in seconds) of a variety of rotating objects observed (or thought to exist, like superstrings which are the mathematical connotation of an elementary particle) in the Universe from the largest to the smallest, are quoted as a function of their radius. Both the inverse frequencies and the radii span 60 orders of magnitude, the relation between the two quantities being almost linear.

the spectrum and angular distribution of the emerging protons, resulting from the stripping of a neutron from the projectile (Fig. 3). The main outcome of these studies, in particular of those carried out on the closed shell nucleus  $^{208}\text{Pb}$ , show that mean-field theory is able, in most cases, to correctly predict the sequence of single-particle levels. However, experiments indicate that the observed density of levels around the Fermi energy is higher than theoretically predicted. It is as if each of the nucleons described by mean-field theory had a mass that is  $\approx 30\text{--}40\%$  smaller than the free nucleon mass. This effective mass is known as the  $k$ -mass [5], indicating the momentum dependence associated with the non-locality in space

of the mean-field (Fock-potential), a feature intimately connected with the fact that nucleons are fermions. Similar effects are found in the case of electrons in metals [6]. Furthermore, the levels lying close to the Fermi energy are less pure single-particle states than mean field theory posits. In fact, the occupation probability of the levels lying below but close to the Fermi energy is not 1 but more like 0.7–0.8. Similarly, levels lying above (and close) to the Fermi energy are not empty as mean field theory predicts, but display occupation factor of the order of 0.2–0.3. Finally, states lying a few MeV ( $\geq 10$  MeV) away from the Fermi energy, display a width (finite lifetime). Mean field theory predicts these states to be sharp.

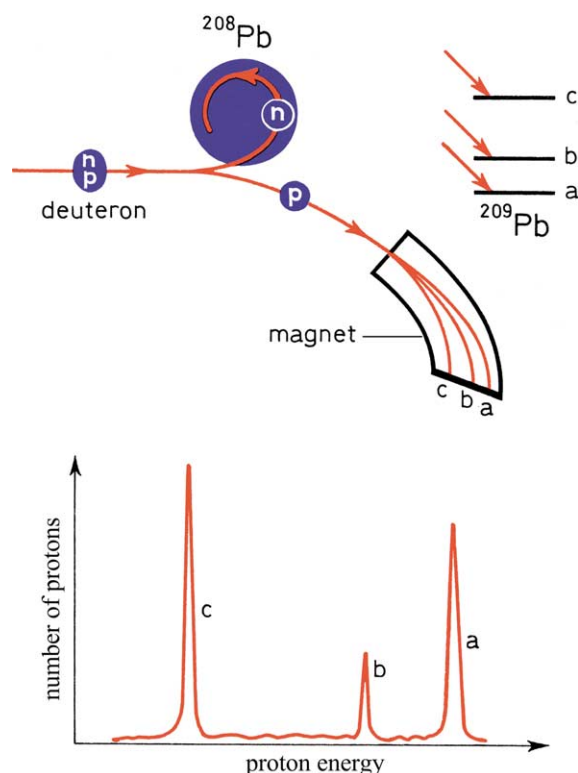


Fig. 3. Nuclear reaction in which a neutron is transferred from the projectile (deuteron) to the nucleus  $^{208}\text{Pb}$ . The energy of the outgoing proton reflects both the  $Q$ -value of the reaction and the energy of the final state of the system.

The limitations mentioned above of mean field theory are connected, in the case of the atomic nucleus, with the fact that one is dealing with a static approximation to the many-particle problem. In fact, the presence of a mean field defines a surface which behaves like that of a liquid drop [7]. That is, as an elastic membrane which, not only confines the motion of the nucleons, but which can also vibrate at different frequencies determined by the surface tension ( $\cong 0.9 \text{ MeV fm}^{-2}$ ) and by the associated inertia of the mode. These vibrations renormalize the properties of the mean field leading, among other things, to an increase in the nuclear radius and diffusivity. Consequently, levels lying somewhat above but close to the Fermi energy  $\epsilon_F$  will decrease its energy coming closer to  $\epsilon_F$ . Levels below (but close to) the Fermi energy will feel two contrasting effects. The increase in the

nuclear radius will decrease their kinetic energy, while the increase in diffusivity will increase it. In any case, the net result is an increase of the density of levels around the Fermi energy.

Microscopically, these results are associated with the fact that a nucleon moving in its orbit can bounce from time to time inelastically off the nuclear surface setting it into vibration. All this costs energy. In fact, surface vibrations require 1–3 MeV to be excited, an energy not available to nucleons moving in levels lying very close to the Fermi energy. According to quantum mechanics, such a violation of energy can happen only for a short period of time, the resulting process carrying the suggestive name of “virtual” process. Consequently, the bouncing of a nucleon inelastically off the nuclear surface has to be repeated a second time in which the nucleon reabsorbs the vibration, eventually returning to its original state (Fig. 4). In this way the particle becomes “dressed”. A dressed nucleon is heavier than a bare nucleon (40–80% heavier), as it has to carry around the vibrations of the nuclear surface to which it couples. In other words, the coupling of the single-particle motion to surface vibrations gives rise to an effective mass (called the  $\omega$ -mass as it depends on the frequency of the vibrational mode), which is larger than the

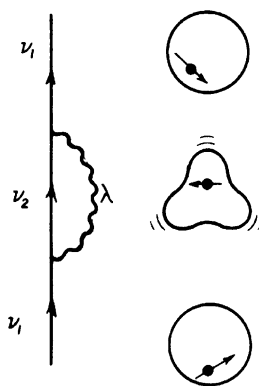


Fig. 4. Lowest-order process by which the single-particle motion is renormalized through the coupling to vibrations of the nuclear surface. The nucleon excites a surface vibration by bouncing inelastically off from the surface and absorbs it again at a later time. Particles are represented by an upwardgoing arrowed line (by a solid dot). The surface vibration is drawn as a wavy line.

bare nucleon mass [5]. The combined  $k$ -mass and  $\omega$ -mass lead to an effective mass that is essentially equal to the bare mass of the nucleon, thus accounting for the observed density of levels at the Fermi energy and the associated occupation probabilities.

A number of nuclear properties, aside from the density of levels at the Fermi energy, depend on the  $\omega$ -mass of the nucleons. In particular the symmetry energy. It is well known that the strong interaction has the same strength acting between all different nucleon species (protons and neutrons). Consequently, protons and neutrons like to be together, and it costs energy to separate them. The symmetry energy quantifies this cost. This energy is made out of two contributions of essentially the same magnitude: a potential and a kinetic energy contribution. The second one depends inversely on the  $\omega$ -mass. Knowledge of the symmetry energy, and thus of the nucleon  $\omega$ -mass is essential in describing such disparate phenomena as the stability and abundance of the nuclear species in the Universe, the occurrence of Super-

novae (the fierce explosions second only to the Big Bang that mark the death of massive stars (cf. e.g. Refs. [8,9])), etc. These examples indicate that the study of the coupling of nucleons to vibrations of the nuclear surface is a subject lying at the forefront of nuclear research, of relevance for a variety of fields ranging from the very small to the very large.

### 2.1.2. Collective motion

Nuclear vibrations are excited by bombarding nuclei with high-energy photons, nucleons, electrons, etc. The vibrations are detected by observing how photons are absorbed by the nucleus, or how protons are scattered inelastically from the nuclear surface, etc. These experiments reveal that the nucleus display both elastic and plastic behaviour. In fact, the so called giant dipole resonance corresponding to a back and forth sloshing of protons against neutrons (Fig. 5(b)), excited in photoabsorption experiments has an energy centroid which scales with the inverse of the radius of the nucleus (a dependence observed for all nuclear

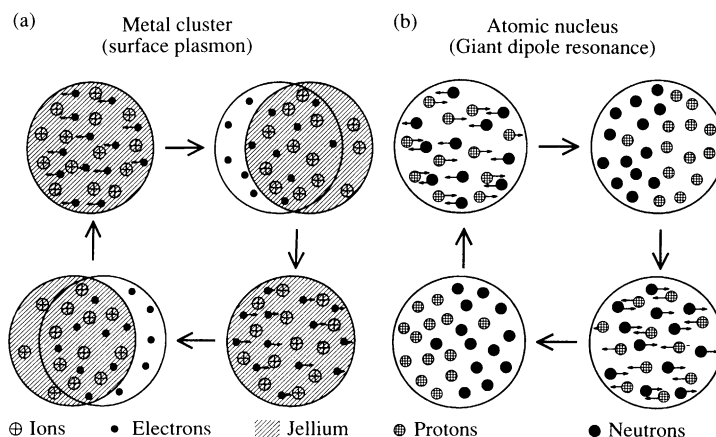


Fig. 5. Schematic representation of the giant dipole resonance in atomic nuclei and of the surface plasmon resonance in small metal clusters. The wavelength of the photon exciting these vibrations is large with respect to the diameter of the system. As a result the electric field associated with a passing gamma ray is nearly uniform across the system. (b) In the case of the excitation of the atomic nucleus, the field exerts a force on the positively charged protons, thus separating them from the neutrons. In fact, the neutrons act as having an (effective) negative charge, which oscillates out of phase with respect to the positively charged protons. (a) In the case of metal clusters, the electric field associated with the photon exerts a force on the positively charged ions and an identical force but with opposite direction on the electrons. Because the ions have a mass which is three orders of magnitude larger than that of the electron, the displacement of the electron cloud is much larger than that of the positive background. Simplified model called the jellium model smears the positive charges of the ions (atomic nuclei) uniformly over the whole volume of the cluster (after Ref. [10]).

resonances), i.e., with the nuclear momentum, a behaviour typical of elastic vibrations. Once excited into a giant dipole resonance the nucleus vibrates at an extremely high frequency, of the order of  $5 \times 10^{21}$  Hz (which corresponds to a vibrational energy of about 20 MeV). To make more vivid the qualification of “extremely” used above, it is useful to remember that the nominal range of human hearing extends from about 20 Hz to  $2 \times 10^4$  Hz, while that of human vision ranges from  $4 \times 10^{14}$  to  $8 \times 10^{14}$  Hz. In order to excite giant resonances with suitable cross sections, use has to be made of fields that change quickly with time, with frequencies of the order of those associated with single-particle motion ( $1/\omega \equiv 10^{23}$  Hz).

The lowest excited states of even–even nuclei display, with very few exceptions, quadrupole and octupole character, that is, they correspond to surface collective vibrations of multipolarity 2 and 3. The associated energies, 1–3 MeV, show a dependence with mass number inversely proportional to the area of the nuclear surface, typical of the vibrations of a liquid drop [7,10]. They reflect the plastic properties of atomic nuclei. In fact, away from closed shells, the energy of the lowest 2+ state can become particularly low in energy (Fig. 6). In these nuclei ( $^{152}\text{Sm}$ ,  $^{154}\text{Sm}$  or e.g.  $^{238}\text{U}$ ), the 2+ state is the lowest member of the so-called ground state rotational band of a spheroidal nu-

cleus rotating around an axis perpendicular to the symmetry axis (Fig. 7). These states are excited with large cross sections by Coulomb and by nuclear fields which change slowly in time ( $1/\omega \equiv 10^{20}$  Hz), as compared with typical frequencies associated with single-particle motion.

Systems displaying both elastic and plastic behaviour are well known from other fields of physics. In particular, the natural caoutchouc, that is, the rubber out of which the tires of cars are made. The basic ingredient of caoutchouc is a liquid, known as latex. It is made out of long polymer chains containing only carbon and hydrogen atoms. When this liquid is boiled together with sulphur, which fixes the polymers among them at certain points, it becomes caoutchouc. In this reaction, only one carbon atom out of 200 of them reacts with the sulphur. Consequently, over long distances the atoms of the polymers occupy reasonably fixed positions, as in a solid, while over short distances they are still quite free to move, as in a liquid. Under a stress, short in time as compared with the diffusion time of the atoms, the liquid part of the material has no time to change place allowing a change in position of the fixed points, and the system reacts elastically, displaying a high degree of elasticity. When the system is subject to an external field over a time of the order or longer than the diffusion time of the polymers,

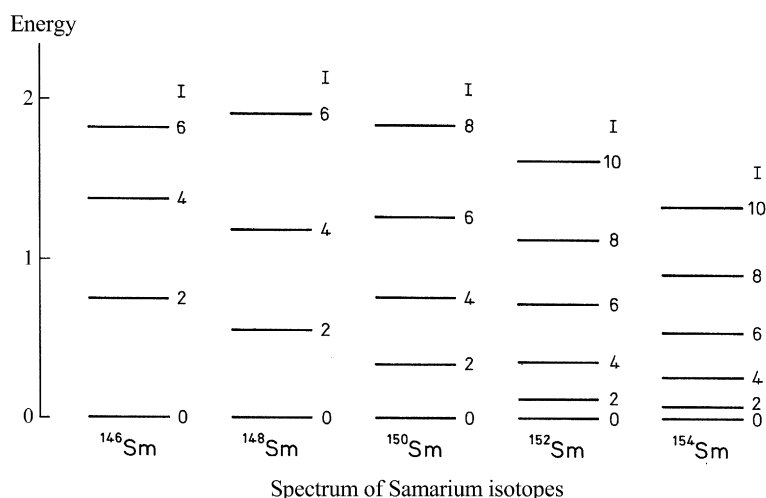


Fig. 6. Sequence of positive parity states of the isotopes of  $_{62}\text{Sm}$ . The energy scale is in MeV.



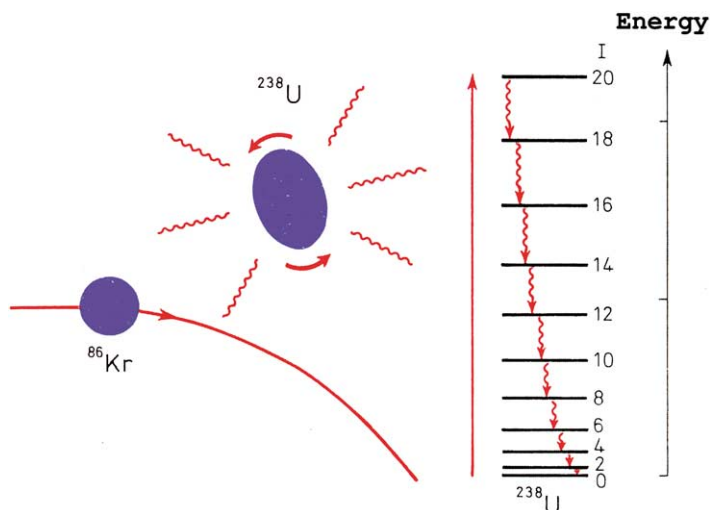


Fig. 7. Excitation of the rotational motion of a (target) nucleus of  $^{238}\text{U}$  by a  $^{86}\text{Kr}$  projectile through the Coulomb field (Coulomb excitation). The system cools down by emitting a number of  $\gamma$ -rays (red wavy arrowed lines) each carrying angular momentum two (in keeping with the quadrupole deformation of the nucleus  $^{238}\text{U}$ ) and different energy, connecting the members of the ground state rotational band of the system.

the fixed points have the possibility to change position in space and the caoutchouc deforms plastically. Evidence of this behaviour in the nuclear case is provided not only by low-lying vibrations and rotations, but also by nuclear fission. This process can be viewed as the division, similar to that of a cell, of a liquid drop into two smaller droplets as a result of deformation (Fig. 8). All

these phenomena are essentially controlled by the nuclear surface.

### 2.1.3. Cooper pairs

The theory describing the coupling of the nucleons to vibrations and to static deformations of the nuclear surface provides an unified description of liquid drop and of independent-particle

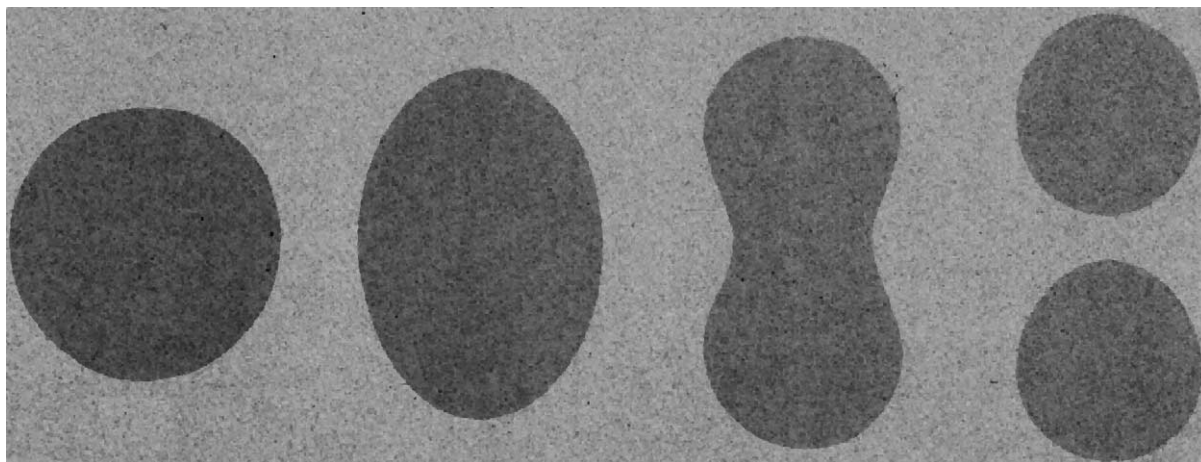


Fig. 8. A schematic sequence of events in the process of spontaneous nuclear fission.

behaviour [11–14]. This unification was crowned with the Nobel Prize in Physics of 1975 given to Aage Bohr, Ben Mottelson and James Rainwater. It constitutes the basis of our present understanding of the atomic nucleus and leads to a number of unexpected effects: neutrons which become charged and protons which weigh more inside than outside the nucleus. Also to the formation of di-neutrons and di-protons which behave like bosons (Cooper pairs) [15]. They can thus undergo Bose–Einstein condensation (BEC). This phenomenon plays a central role in determining the properties of nuclei close to the ground state, in particular nuclear rotation.

The rotational motion is one of the simplest and, at the same time, most profound examples of periodic motion (think only on the earth rotation around itself and around the Sun and on the succession between day and night and between summer and winter). A detailed study of the rotational frequency and of the variations of the rotational period as a function of time can provide important information on the physical properties of the system under study and on the forces acting inside it. Confronted with two eggs lying on the kitchen table, one of which we have been told has been hard boiled and the other not, one does not need to break them open to learn which of the two is cooked. It is sufficient to make them rotate by spinning them. One of the two will rotate for quite a while almost undisturbed, while the other one will stop rotating already after few revolutions. Obviously, the first of them is the hard boiled egg.

Strongly rotating nuclei (Fig. 2) can be produced in the laboratory either via Coulomb excitation (Fig. 7) or in fusion processes (Fig. 1). Because the system is charged, the rotating nucleus emits “light”, that is gamma rays which provide detailed information on the properties of the system. A surprising result emerging from such measurements is that at low rotational frequencies, the moment of inertia of the system is considerably smaller, about half than the expected (rigid) moment of inertia, while at higher rotational frequencies the moment of inertia coincides more or less with the rigid moment of inertia of the system. It is as if at low rotational frequencies the nucleus behaves like a raw egg, while it spins like a hard-

boiled egg at high rotational frequencies. The explanation of this unexpected behaviour is also surprising: the nucleus, which in connection with the present discussion can be viewed as a spheroidal container, is filled at low rotational frequencies with a non-viscous (superfluid) liquid. Spinning the container, only the matter at the poles, that is, the matter directly pushed by the walls (surface) of the container is set up into motion, the central core remaining at rest (Fig. 9). On the other hand, at high rotational frequencies the nucleus displays a phase transition into a system of nucleons moving independently of each other in well defined orbits (normal system). Each of these orbits are solidly anchored to the mean field (surface) of the nucleus. Consequently, each nucleon inside the nucleus reacts to a change in the rotational frequency with its full mass. The collective motion of the system thus coincides with that of a rigid body of the same mass, dimension, and deformation of the nucleus under study.

These phenomena are closely connected with the variety of effects belonging to the field of low-

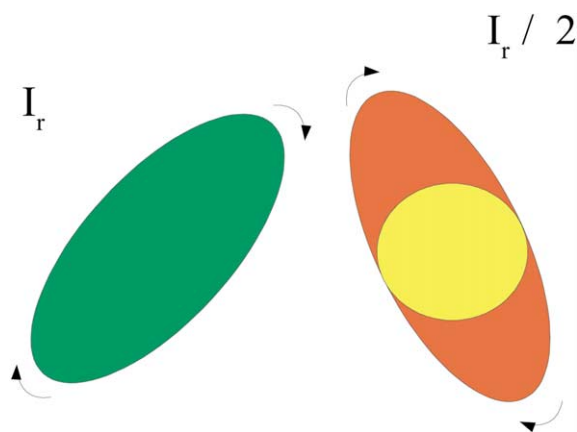


Fig. 9. Schematic representation of the reaction to rotation of a deformed nucleus. In the left part of the figure it is assumed that the system can be described in terms of the motion of independent nucleons (fermions). The associated moment of inertia is equal to the rigid moment of inertia  $I_r$ . In the right part of the figure it is assumed that the system is filled with a superfluid fluid (made out of pairs of fermions) displaying no friction. Consequently, under rotation the central core (yellow) remains essentially at rest and only the matter associated with the poles (orange) is involved in the rotation. The associated moment of inertia of this system is  $\approx I_r/2$ .

temperature physics, which go under the name of “superconductivity” [15,16] when they occur in an electric charged system such as electrons in a metal, and “superfluidity” when they occur in a neutral system such as an insulating liquid [17]. The behaviour of a superconducting metal is qualitatively different from that of a normal metal, in that it conducts electricity with zero resistance (hence the name). Similarly, a liquid that goes superfluid can flow through tiny capillars without apparent friction, and can even climb up over the rim of a vessel containing it and thereby gradually empty the vessel.

The importance of the subject has been acknowledged by the Swedish Royal Academy of Sciences with a host of Nobel Prizes in Physics (1913, 1962, 1972, 1973, 1978, 1987, 1996).

## 2.2. Bose–Einstein condensation

To sketch the general picture, let us concentrate on the common isotope of helium ( $^4\text{He}$ ). Such an atom has zero total spin, and therefore, according to quantum mechanics should obey Bose–Einstein statistics. Consequently, when a large number of such particles are placed in a restricted volume and are cooled down below a certain temperature (which for helium turns out to be about 3 K), a phenomenon called BEC takes place: namely, a finite fraction of all the atoms begins to occupy a single quantum-mechanical state, the fraction increasing as the temperature decreases. Thus, in the same way that fermions are extremely individualistic, each of them occupying a different (quantal) state, bosons are extremely gregarious and love to be in the same (quantal) state of the system. The atoms in this special situation become locked together in their motion, like soldiers in a well drilled army, and can no longer behave independently. Thus, for example, if the liquid flows through a narrow capillary, the processes of scattering of individual atoms by roughness in the walls, which would produce so strong a viscous drag on any normal liquid as to effectively prevent it from flowing at all, is now quite ineffective, since all atoms (bosons) must scatter or none.

A similar picture applies to superconductivity in metals. However, in this case the “particles” that

undergo BEC (and are therefore required to be bosons) are not individual electrons, which have spin  $1/2$  and are fermions. The “particles” are pairs of electrons (Cooper pairs) which form in the metal, and carry mass and charge double of that of a single electron aside from total spin zero. Cooper pairs condense when the metal is cooled down (e.g. below 7 K in the case of lead) and occupy a single quantal state. A similar phenomenon takes place in the nuclear case, where pairs of nucleons moving in time reversal states form Cooper pairs with total angular momentum zero (Fig. 10). Because the nucleus in its ground state or in the states belonging to the so called yrast band (that is the states of lowest energy for a given angular momentum, where all the energy of excitation is tied up in the collective, ordered rotational motion of the system as a whole) is at zero temperature, these Cooper pairs condense, giving rise to a superfluid non-viscous liquid.

The variation of the rotational frequency of deformed nuclei displays sharp discontinuities (Fig. 11). This phenomenon reflects the fact that rotation has opposite effect on the motion of the two members of each Cooper pair (Fig. 12). After a compound nucleus, with high angular momentum and excitation energy, has been formed in a fusion process, it cools down by evaporating particles. When the excited nucleus comes close to or eventually reaches the yrast line, it continues to slow down by emitting gamma rays each carrying two units of angular momentum. At the beginning of this process, the rotational frequency is so high that the associated energy is larger than the binding energy of each pair. Consequently no Cooper pair is present in the system, and the nucleus behaves as a normal system displaying a rigid moment of inertia. As the nucleus continues to decrease its rotational frequency it will eventually arrive at a (critical) frequency below which pair formation can take place, and the system can make a transition to the superfluid phase. Consequently, the moment of inertia of the system decreases by a factor of  $\approx 2$ . The rotational frequency thus increases sharply. This is because the product of the moment of inertia and the rotational frequency is equal to the total angular momentum of the system, a quantity which is conserved. Thus, the

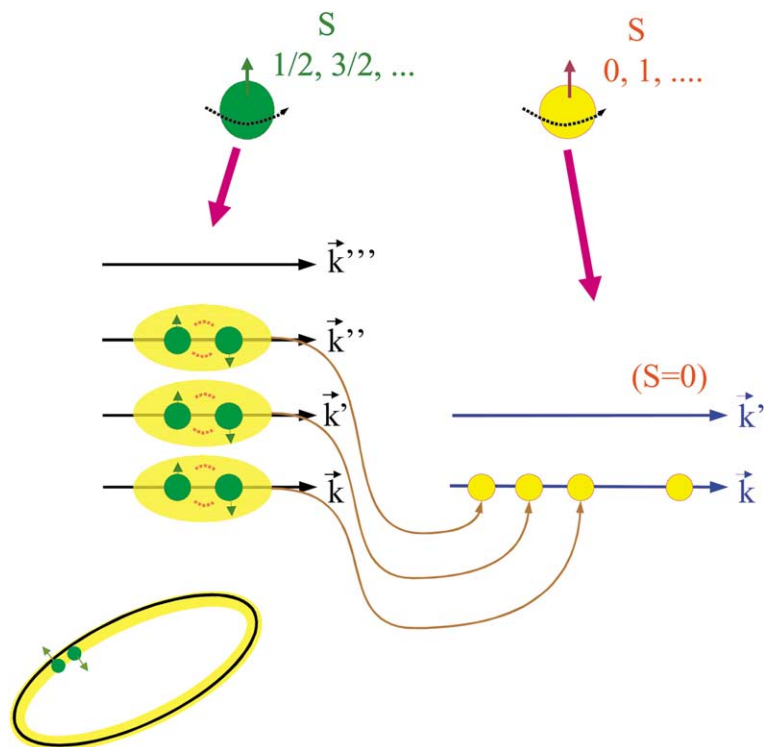


Fig. 10. Particles displaying half-integer values of the spin are called fermions, fulfill Fermi–Dirac statistics and according to the exclusion principles cannot occupy the same quantal state labeled in the figure by the quantum number  $\vec{k}$  and by the intrinsic spin which can be in one of two states, namely spin up and spin down, associated with the two projections ( $\pm 1/2$ ) of a spin  $s = 1/2$  as that of the nucleon or of an electron, and explicitly shown in the figure in terms of an arrow pointing up or down respectively. Particles of integer spin are called bosons and fulfill Bose–Einstein statistics. They can all occupy the same quantal state. Coupling two fermions to integer spin, e.g.  $S = 0$ , one can form a boson (Cooper pair). If the temperature of the system is lower than the binding energy of the Cooper pair, a condensation phenomenon can also take place in this case. In nuclei the interaction responsible for the formation of Cooper pairs can be viewed as a surface phenomenon effect (cf. also Fig. 13).

observed discontinuities in the decrease of the rotational period is intimately related with the normal–superfluid phase transition taking place as a function of the rotational frequency. This transition is associated with a violent variation of the moment of inertia of the system, that is, to a nuclear quake.

In the case of low-temperature superconductivity the attraction among electrons is generated by the exchange of lattice phonons between them (and the energy needed to break the pair is of the order of few milli ( $10^{-3}$ ) electron volts). In the nuclear case, roughly 50% of the pairing effects is due to a phenomenon similar to this one, namely the exchange of collective surface

vibrations between nucleons [18]. The other 50% is due to the strong force acting between nucleons and arising from the exchange of mesons (the carriers of the strong force) between nucleons (cf. Fig. 13). The effect this force has on nucleons moving in states connected by the operation of time reversal (Fig. 12) can be measured in scattering process between nucleons and expressed in terms of the  $^1S_0$  phase shift (cf. Fig. 13 and corresponding caption). It is found that the exchange of mesons leads to a pairing force which is attractive at low relative momenta, that is in situations similar to that experienced by pairs of nucleons moving on the surface of the nucleus.

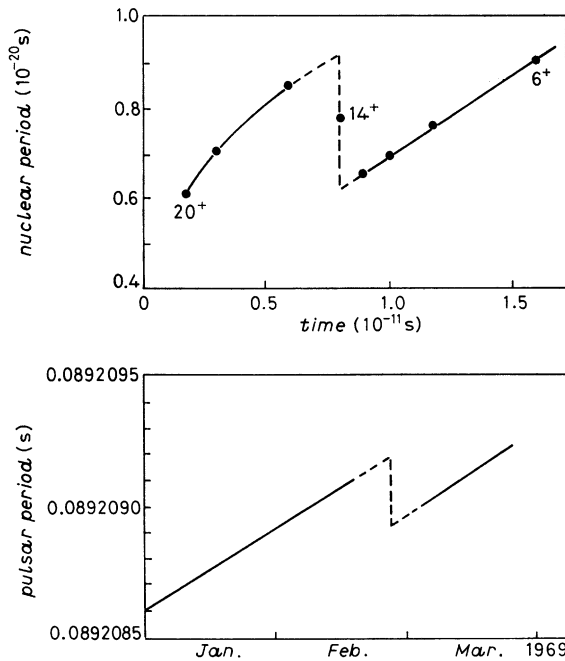


Fig. 11. Plot of the rotational period versus time for the nucleus  $^{158}\text{Er}$  (top) and the pulsar Vela (bottom).

The role the exchange of nuclear surface vibrations has on Cooper pair formation is larger for small rather than for large nuclei. This is because the surface–volume ratio, and thus the curvature of the system as well as the spill out of nucleons is larger for the light nuclei. Consequently, in these systems the collectivity of surface vibrations is larger than in the heavier systems. These effects become exacerbated in the case of very light exotic nuclei (cf. next subsection). We shall also see that effects similar to these open the possibility of creating real high  $T_c$  superconductors when applied to the case of fullerene based materials (cf. Section 2.4).

The central role played by the surface in the condensation process leading to nuclear superfluidity, where nucleons move without friction, is demonstrated by the fact that BEC essentially happens only at the surface of the nucleus. In other words, nucleons behave in the nuclear surface like a superfluid, while inside the nucleus they display normal properties, including friction. The pairing

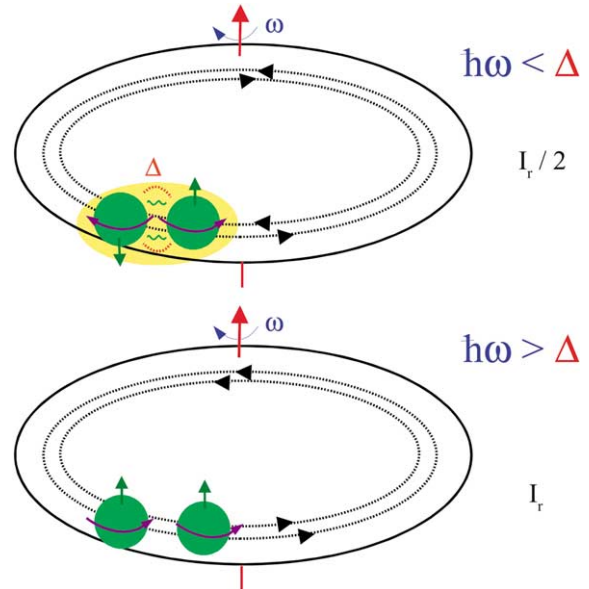


Fig. 12. Pair of nucleons moving in states of time-reversal (clockwise and anticlockwise, spin up and spin down) and forming a Cooper pair in a deformed nucleus which rotates as a whole with frequency  $\omega$ . The binding energy of the pair is measured by the quantity  $\Delta$ , known as the pairing gap [15], the interaction among the nucleons being represented by red dotted curves and green wavy lines (see also Fig. 13). For rotational frequencies such that the rotational energy  $\hbar\omega$  is smaller than the pairing gap (top), the system behaves as a condensate of Cooper pairs (bosons), with the moment of inertia being one half the rigid moment of inertia (cf. Fig. 10). For rotational frequencies such that  $\hbar\omega$  is larger than  $\Delta$ , the nucleon moving clockwise in its trajectory is so much retarded in its revolution period with respect to the partner nucleon, that it cannot correlate efficiently any more with it and “align” its motion (and spin) with the rotational motion, becoming again a pair of fermions and not participating any more in the condensate (cf. Fig. 11).

gap [15], the energy which provides a quantitative measure of the binding energy of the Cooper pairs and thus of the superfluidity of the system, is large ( $\approx 1$  MeV) at the nuclear surface, becoming essentially zero inside the nucleus.

### 2.3. Exotic forms of nuclear matter

Surface controlled pairing is also believed to be responsible for the existence of exotic forms of nuclear matter at very low densities. These so

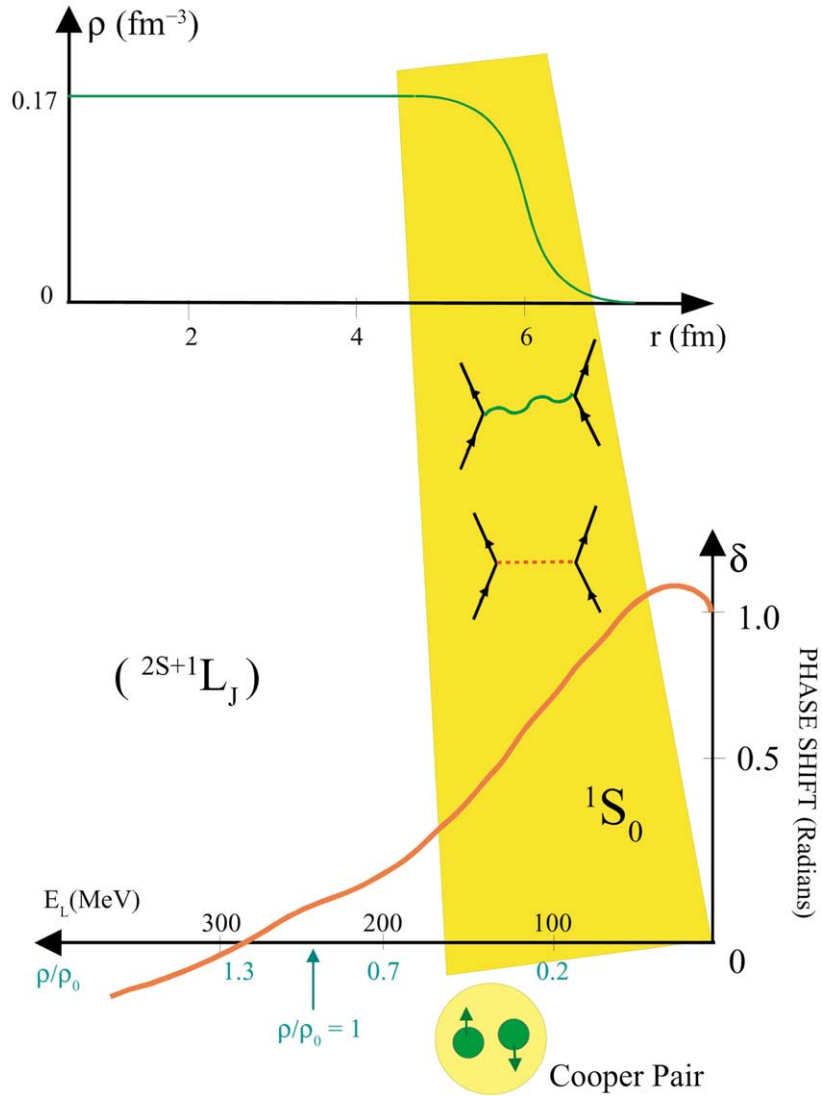


Fig. 13. (top) Nuclear density  $\rho$  in units of  $\text{fm}^{-3}$  (where  $\text{fm} \equiv 10^{-13}$  cm), plotted as a function of the distance  $r$  (in units of fm) from the centre of the nucleus. Saturation density corresponds to  $\approx 0.17 \text{ fm}^{-3}$ , equivalent to  $2.8 \times 10^{14} \text{ g/cm}^3$ . Because of the short range of the nuclear force, the strong force, the nuclear density changes from 90% of saturation density to 10% within 0.65 fm, i.e. within the nuclear diffusivity. (bottom) Phase parameter associated with the elastic scattering of two nucleons moving in states of time reversal, so called  $^1S_0$  phase shift, in keeping with the fact that the system is in a singlet state of spin zero. The solution of the Schrödinger equation describing the elastic scattering of a nucleon from a scattering centre (in this case another nucleon) is, at large distances from the scattering centre a superposition of the incoming wave and of the outgoing, scattering wave. The interaction of the incoming particle with the target particle changes only the amplitude of the outgoing wave. This amplitude can be written in terms of a real phase shift—or scattering phase— $\delta$ . Positive values of  $\delta$  implies an attractive interaction, negative a repulsive one. For low relative velocities (kinetic energies  $E_L$ ), i.e. around the nuclear surface where the density is low, the  $^1S_0$  phase shift arising from the exchange of mesons (like for example pions, represented by an horizontal dotted red line) between nucleons (represented by upward pointing arrowed lines) is attractive. This mechanism provides about half of the glue to nucleons moving in time reversal states to form Cooper pairs. These pairs behave like boson and eventually condense in a single quantal state leading to nuclear superfluidity. Cooper pair formation is further assisted by the exchange of collective surface vibrations (green wavy curve in the scattering process) between the members of the pair.

called halo nuclei, which lie at the limits of stability of the chart of nuclides [19] (cf. Fig. 14), are composed of essentially all surface and display a very large spill out of nucleons.

### 2.3.1. Halo nuclei

These nuclei exist at the neutron drip line in the chart of nuclides (see below and Fig. 15(B)) and their study constitute one of the most important subjects lying at the forefront of nuclear research.

When neutrons are progressively added to a normal nucleus, the Pauli principle forces them into states of higher momentum. When the core becomes neutron-saturated, the nucleus expels most of the wavefunction of the last neutrons outside to form a halo, which because of its larger size can have lower momentum. In most cases neutrons essentially drip off from the nucleus, defining the lines of stability for neutron number in the chart of nuclides (neutron drip line, cf. Fig. 15(B), dashed lines marked  $B_n = 0$ ). In some few, selected cases, the system becomes a halo nucleus. In halo nuclei, some of the constituents neutrons venture beyond the drop's surface and form a misty cloud or halo (similar effects are found for nuclei close to the proton drip line, cf. Fig. 15(B) dashed lines marked  $B_p = 0$ ). Not surprisingly, these extended nuclei behave very differently from ordinary ("normal") nuclei lying along the stability valley in the chart of nuclides. In particular, they are larger than normal nuclei of the same mass number. For example,  $^{11}\text{Li}$  is twice as large as  $^{11}\text{B}$ , a stable nucleus containing the same number of nucleons and half the size of the lead nucleus  $^{208}\text{Pb}$ , which holds 197 more particles (Fig. 14). In the case of  $^{11}\text{Li}$ , the last two neutrons are very weakly bound. Consequently, these neutrons need very little energy to move away from the nucleus. There, they can remain in their "stratospheric" orbits, spreading out and forming a tenuous halo. If one neutron is taken away from  $^{11}\text{Li}$ , a second neutron will come out immediately, leaving behind the core of the system, the ordinary nucleus  $^9\text{Li}$ . This result indicates that pairing may play an important role in the stability of  $^{11}\text{Li}$ . In fact, the properties of the exotic nucleus  $^{11}\text{Li}$  can be understood, even quantitatively, in terms of the simplest scenario imaginable: the formation of a

single di-neutron Cooper pair which is held together to the  $^9\text{Li}$  core essentially by the exchange of surface vibrations among the halo nucleons (Fig. 15(A)) [21]. The importance of these vibrations is due to the high polarizability displayed by  $^{11}\text{Li}$  [20].

Current research in nuclear physics and astrophysics focuses on exploring the behaviour of nucleonic matter under the extreme conditions associated with the drip lines (surface dominated nuclei). For this purpose, use is made of beams of new nuclear species created in modern accelerator laboratories [22]. To be noted that of all the atomic nuclei which are thought to be possible, only about half of them have been observed in the laboratory, and a small fraction exist naturally on Earth (cf. Fig. 15(B)). Of particular importance in this research are the mechanism for the creation of elements in the Universe. Unstable nuclei are involved in explosive burning in astrophysical environments. Prominent among these processes are explosive hydrogen burning (the rp-process) on the surface of accreting white dwarfs (novae) or neutron stars (X-ray bursts), as well as rapid neutron capture (the r-process) in very neutron-rich conditions of Supernova explosions (cf. Fig. 16). The r- and rp-process paths shown in Fig. 15(B), traverse regions of unstable nuclei of the chart of nuclides which are as yet unexplored. A third path, the s-process path, runs along the stable nuclei.

### 2.3.2. Neutron stars

The nuclear surface controls not only the properties of individual nuclei, but also the properties of "materials" whose building blocks are atomic nuclei. These femtometre materials display properties reflecting not only the ubiquitous role played by the interweaving of nucleons and surface vibrations, but also the marked dependence of the strong force with density. A textbook example is provided by neutron stars (pulsars) [23]. These remnants of fierce Supernova explosions are gigantic, rapidly rotating nuclei thirty kilometers across, held together by the gravitational force (Figs. 16 and 17), a discovery which led in 1974 to the Nobel Prize in physics for Anthony Hewish [26]. Neutron stars display, in the process of cooling down through radiation and particle



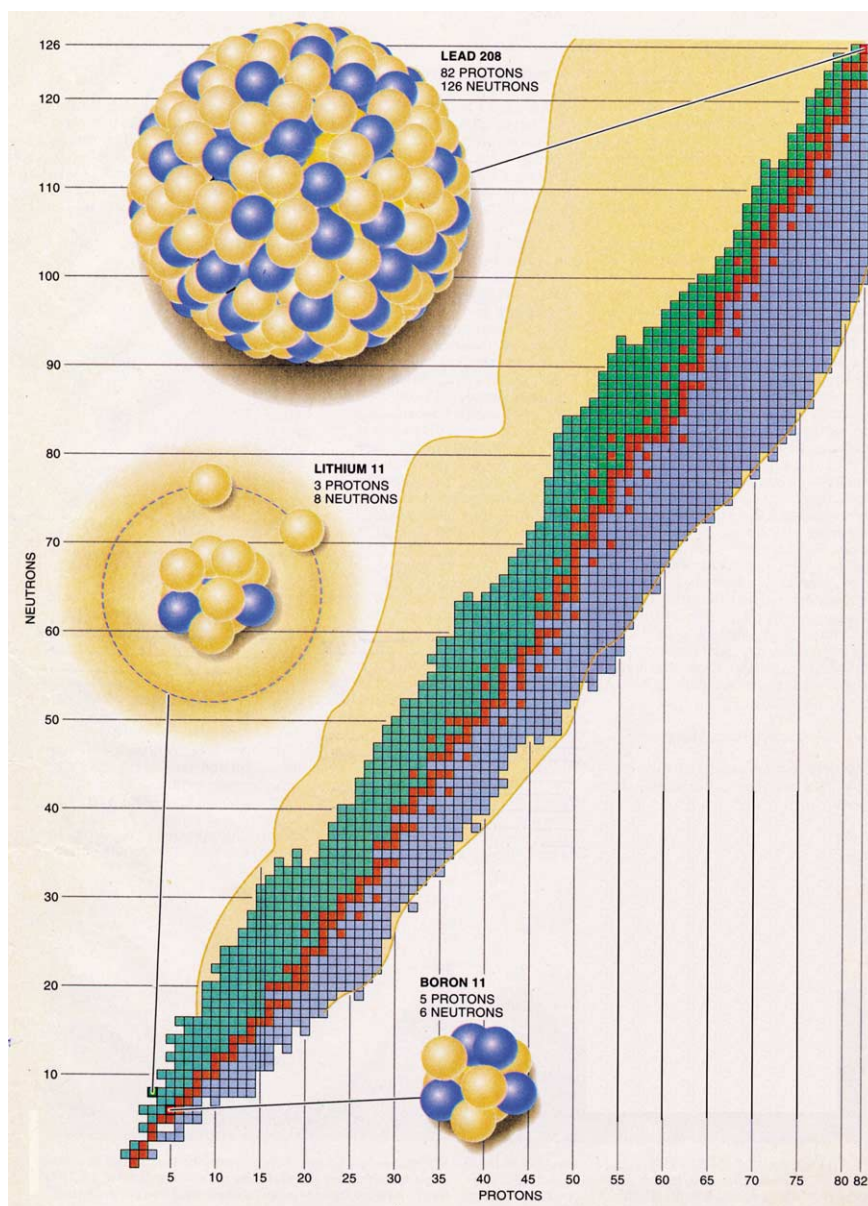


Fig. 14. Nuclei are represented here by squares, positioned horizontally according to the number of protons and vertically according to the number of neutrons they contain. Stable nuclei are shown as gold squares. Green squares indicate bound but unstable nuclei that have excess neutrons. Blue squares mark bound, proton-rich nuclei. The outer borders of these regions are called drip lines, along which large halo nuclei may be found. The extended halo of lithium 11, comprising two neutrons, makes this nucleus nearly twice as large as boron 11, a stable nucleus containing the same number of nucleons.  $^{11}\text{Li}$  is half the size of a lead nucleus that holds 197 more particles,  $^{208}\text{Pb}$  (after Ref. [19]).

emission, marked glitches (starquakes) (Fig. 11), which are likely to be connected with di-nucleon

BEC [24,25]. In fact, neutron stars usually rotate with such precision that they are known as the best



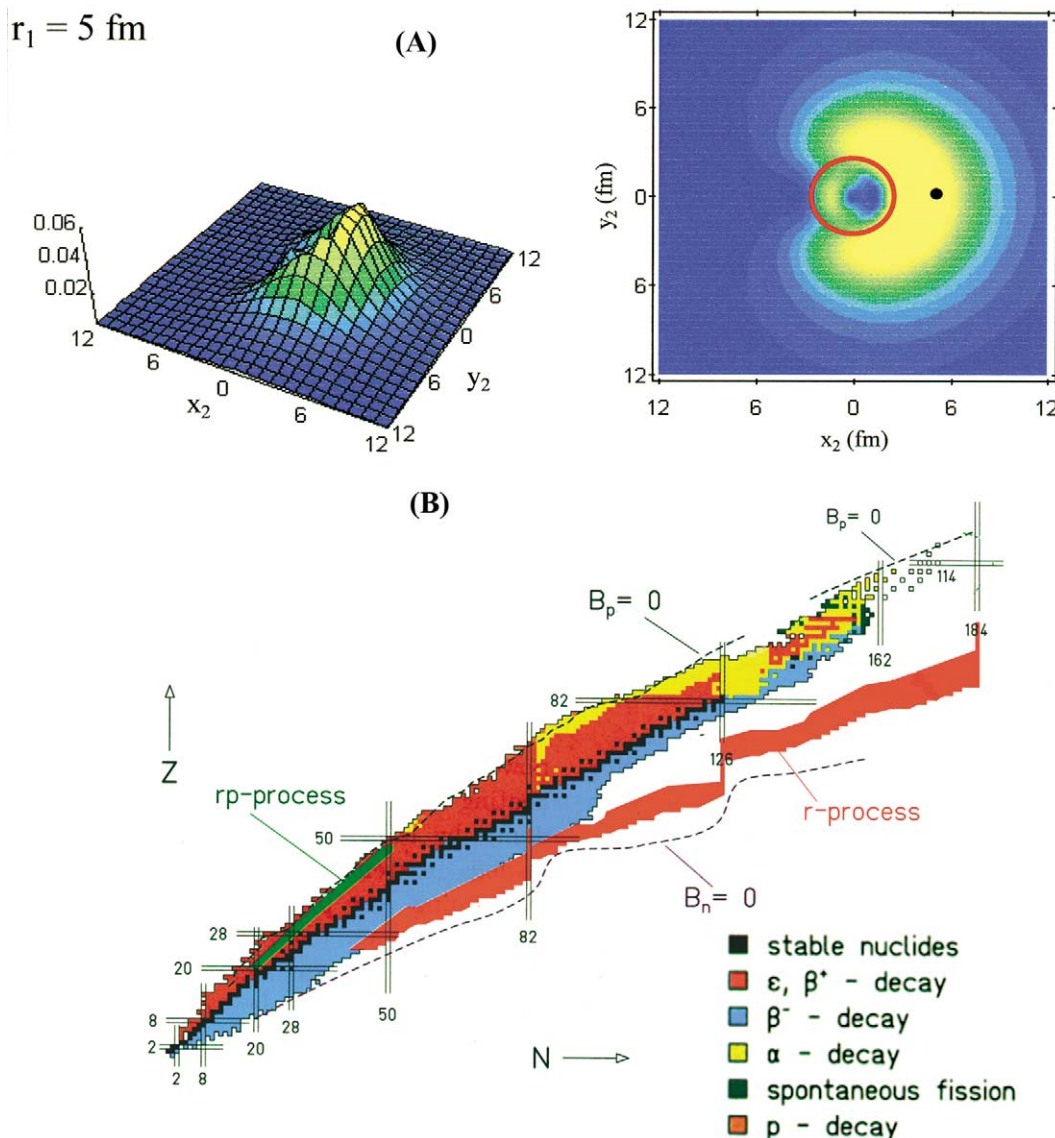


Fig. 15. (A) Spatial structure of the Cooper pair which describes the two halo neutrons of  ${}^{11}\text{Li}$  [21]. Fixing one of the two neutrons at a distance of 5 fm from the origin of the nucleus (black dot) on the  $x$ -axis, the probability of finding the other neutron is displayed. The numbers appearing on the  $z$ -axis of the three-dimensional plot displayed to the left side are in units of  $\text{fm}^{-2}$ . The projection on the  $x$ - $y$  plane is shown on the right panel, where the core  ${}^9\text{Li}$  is shown as a red circle. (B) Map of the nuclear landscape, as in Fig. 14, where particular characteristics which makes it easier to appreciate the new area of research associated with exotic nuclei are emphasized. The nuclei existing naturally on Earth are marked by black squares. The magic numbers associated with increased stability (closed shells), are the convenient “landmarks” in the map and are indicated by double lines. Also shown are estimates of the borderline of stability, the so called drip lines, where the proton and neutron binding energies  $B_p$  and  $B_n$  become zero. Also shown are two paths astrophysicists identify as important in the creation of elements in the Universe: the  $r$ -process and the  $rp$ -process which transverse regions yet unexplored. A third path, the  $s$ -process path, runs along the stable nuclei.

time keepers in the Universe. But every so often their rotation rate increases. It is thought that

these glitches are related to superfluidity inside the star, in particular superfluidity in the inner crust of

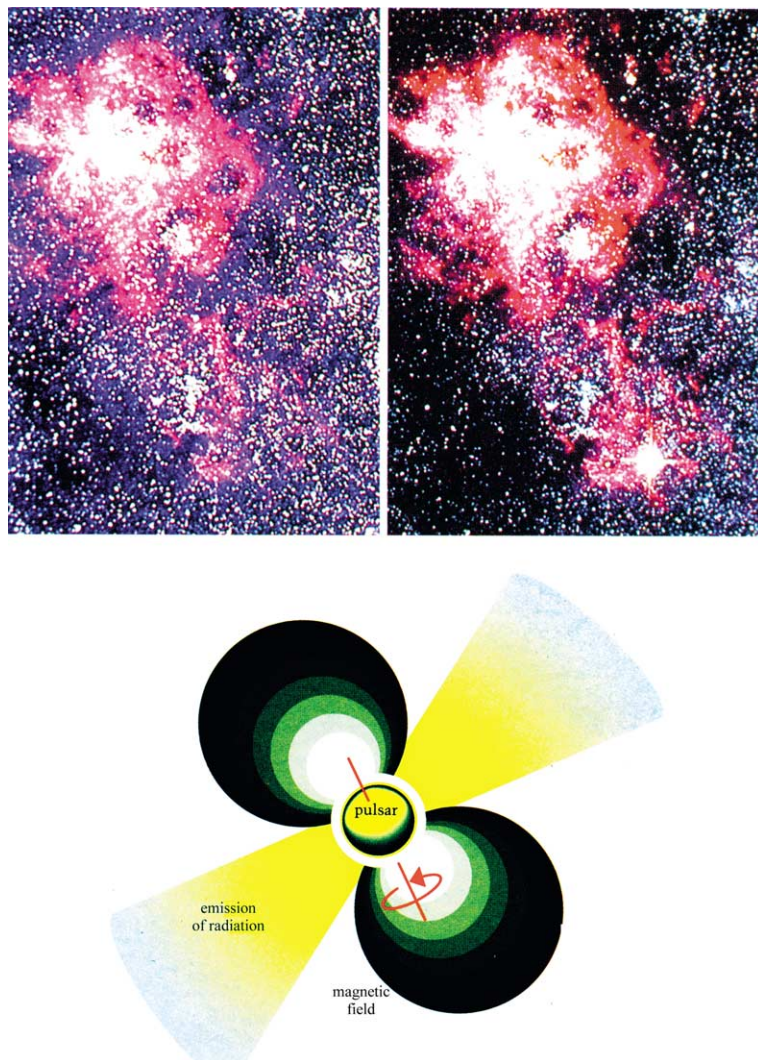


Fig. 16. On February 23, 1987, the great Magellanic cloud was the scene of a supernova explosion. Supernova 1987A as it was christened was so bright that one could see it from the Southern hemisphere and during a period of about six months with the naked eye. (top) A photo of the Magellanic cloud before (left) and after (right) the date indicated above. A bright spot on the lower part of the figure is clearly visible. (bottom) Neutron stars have an intense magnetic field which accelerates electrons and protons, inducing those particles to emit beams of radiation. These beams arrive to the earth with a frequency determined by the rotation of the star giving rise to a pulsating signal like light emitted by a lighthouse. Hence, the name pulsar.

the star, where nuclei forming a crystalline lattice are immersed in a sea of free, superfluid neutrons. Because a superfluid can rotate only by forming (quantized) vortices, the coexistence of superfluid neutrons and lattice nuclei in the crust leads to a special rotational dynamics. In it, vortex lines become pinned to the normal (bulk) nucleons of nuclei forming the lattice, where the pairing gap

is small. Pulsar glitches are thought to be caused by the sudden release of pinned vortex lines [27] which eventually hit the outer surface of the star making it spin faster. The detailed understanding of these phenomena for the hundreds of pulsars known in the Universe, constitutes a subject lying at the forefront of astrophysical research.

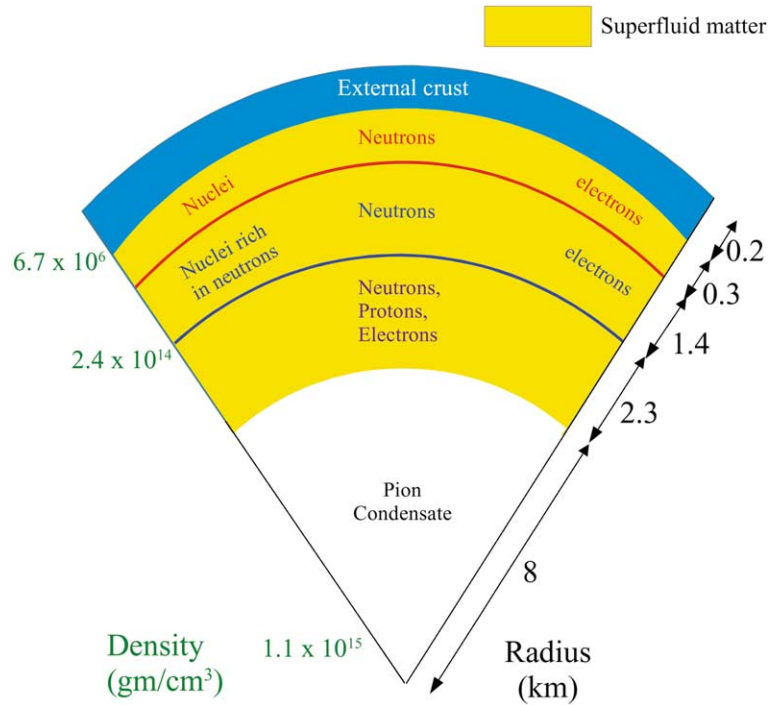


Fig. 17. Cross-section of a neutron star calculated making use of a so called stiff equation of state for neutron matter densities larger or equal than nuclear saturation density [23].

### 2.3.3. Femtometre materials

A Gedanken experiment designed to measure the electrical resistivity of a femtometre wire of the material filling the inner crust of a neutron star, but where neutrons are replaced by protons, will reveal a superconductor. In particular, let us think of a femtometre wire made out of  $^{210}_{84}\text{Po}_{126}$ , a nucleus with two protons moving outside the doubly closed shell system  $^{208}_{82}\text{Pb}_{126}$  (with “magic numbers” of both protons (82) and neutrons (126), cf. Fig. 14). This nucleus displays a pairing gap (i.e. a binding energy of the Cooper pair) of the order of 1.2 MeV, arising from the nuclear pairing interactions (strong force and exchange of surface vibrational modes) strongly concentrated on the nuclear surface. If one could create a crystal where the average distance between each  $^{210}\text{Po}$  nucleus was of the order of 15 fm, so that the distance between the surface of each nucleus was about 1 fm, one would produce a real high  $T_c$  superconductor. In fact, each nucleus will contribute a

strongly correlated two proton Cooper pair to the conducting band. While the density of levels at the Fermi energy is expected to be somewhat lower than that associated with the single nucleus, one could still expect a pairing gap of the order of hundreds of keV.

### 2.4. Analogies: nanometre materials

While it is not possible to produce bulk samples of femtometre materials in the laboratory, one can recognize that the mechanism which is at the basis of this ideal material, namely superconductivity controlled by pairing interactions mediated by the surface of each single atomic nucleus and the density of levels of the whole crystal, is that which seems to be active in so called high  $T_c$ -superconductors made out of doped fullerenes. In these materials, the protons are replaced by electrons while the nuclei forming the Coulomb lattice of the inner neutron star crust, the building blocks of the

material, are replaced by the soccer ball-like carbon molecule  $C_{60}$  [28], the brilliant discovery of Robert F. Curl and Richard E. Smalley of Rice University and Harold W. Kroto of the University of Sussex for which they were awarded the 1996

Nobel Prize in Chemistry. The Cooper pairs are, in these materials, thought to be formed by the exchange, between pairs of electrons of the doping atoms, of intraball ( $C_{60}$ ) surface vibrations (phonons) [29] (Fig. 18).

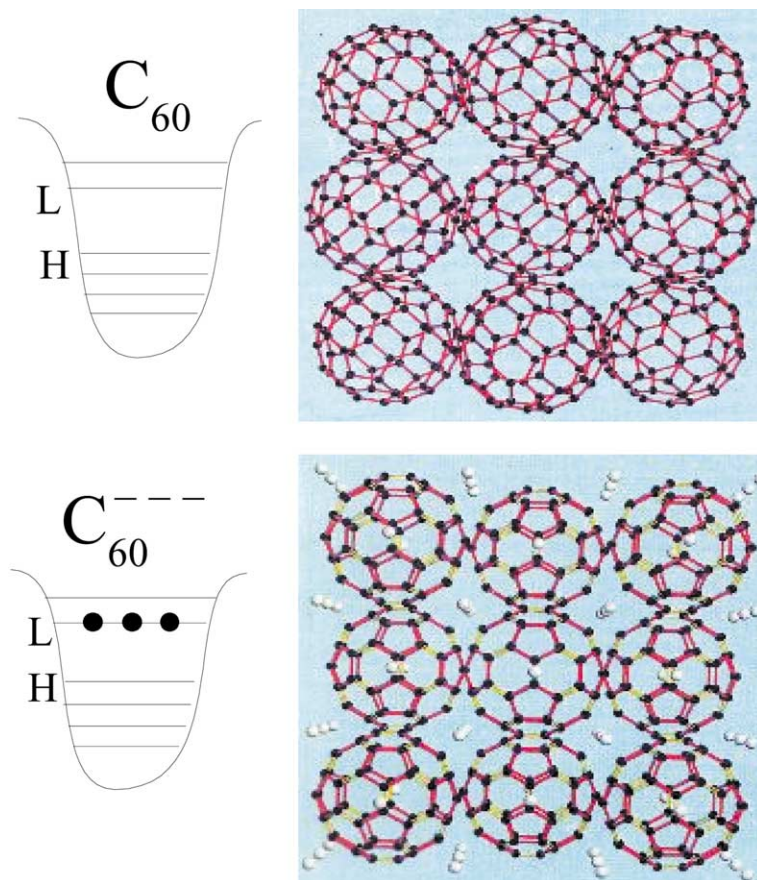


Fig. 18. (top) Model illustrating the packing of individual fullerenes clusters in the fcc lattice of solid  $C_{60}$ . (bottom) Model illustrating the packing of alkali metal ions into the tetrahedral and octahedral holes in the fcc  $C_{60}K_3$  lattice (K stands for potassium but other alkali metals like Rb and Cs have been used to dope  $C_{60}$  solid leading to superconducting systems [29,75]). In the top, we schematically show the potential in which the electrons of  $C_{60}$  move leading to a “closed shell” system, that is, a system of fermions where all levels are completely filled up to the highest occupied molecular orbital (HOMO) and there is a “large” gap, of the order of a couple of electron volts between this level and the lowest unoccupied molecular orbital (LUMO). This is the reason why solid  $C_{60}$  is an insulating material. If one adds electrons to  $C_{60}$ , e.g. three electrons leading to  $C_{60}^{--}$  (bottom) they can correlate by exchanging vibrations of the molecule, and form Cooper pairs. However, because of the fact that the dimension of the Cooper pair is larger than the  $C_{60}^{--}$  system it cannot display a supercurrent. This can develop in e.g. a solid  $C_{60}K_3$ , where still the glue between the electrons is provided by the intramolecular vibrations, but where the size of the sample is much larger than the dimensions of the Cooper pair. To be noted that the glue between electrons in low-temperature (metallic) superconductors is provided by the intermolecular vibrations of the atoms of the crystal lattice. Due to the symmetries of the molecule  $C_{60}$ , its LUMO has degeneracy six, that is, it can accommodate six electrons, three with spin up and three with spin down. This is the reason why three metallic atoms (each providing one electron) are used to dope solid  $C_{60}$ , as the largest pairing correlations are obtained for a half filled (narrow) band.



These vibrations are much more effective in providing a glue between pairs of electrons than those associated with graphite. In fact, the critical temperature  $T_c$ , below which the system is superconductor is  $T_c \equiv 5$  K for graphite compounds and  $T_c \equiv 112$  K for hole doped  $C_{60}$  fullerite [30]. Because  $C_{60}$  can be viewed as made out of a wrapped carbon lattice plane by introducing defects in the honeycomb lattice so as to create 12 pentagons ( $C_{60}$  is made out of these 12 pentagons and of 20 hexagons), curvature effects and electron spill out seems to be at the basis of the increased electron–phonon coupling observed in going from graphite to  $C_{60}$ -based materials [31]. It is thus expected that materials made out of fullerenes with higher curvature and electron spill out than  $C_{60}$ , like  $C_{36}$ ,  $C_{28}$  and  $C_{20}$  will display higher values of  $T_c$  [32,33]. This can be accomplished by reducing the number of hexagonal faces of the cage as one cannot reduce the number of pentagons. This is because according to Euler’s theorem, 12 is the minimum number of pentagons a polyhedron can have. Therefore  $C_{20}$ , which is made out of exactly 12 pentagons, is the smallest of the family of fullerenes, displaying the largest surface to volume ratio. Consequently also the largest curvature and, potentially, the largest electron spill out. The associated phonons are thus likely to provide the strongest glue between pairs of electrons in fullerene based materials. While  $C_{20}$  fullerenes have recently been made using a gas-phase reaction method [34], no solid using this molecule as building block has yet been produced. Assuming that a  $C_{20}$  based solid can be made (which although covalent preserves the identity of the individual molecules) displaying a density of levels at the Fermi energy similar to that of the alkali doped  $C_{60}$  fullerite mentioned in connection with Fig. 18, one could expect a critical temperature  $T_c$  about eight times higher than that associated with  $A_3C_{60}$  [33]. In other words, one could expect essentially a room temperature superconductor.

To assess the validity of such possibilities one would need to understand in detail at least three main issues concerning fullerene based materials: (a) the electron–phonon coupling in a strong coupled situation (in particular for small fullerenes); (b) the screening of the Coulomb field

which essentially amounts to understanding in detail the electron–plasmon coupling; and (c) the modifications of these properties in the solid. It is likely that such research may contribute not only to shed light on fullerene based materials, but also on high  $T_c$  superconductors at large [35].

Curvature, and thus surface driven superconductivity may also be encountered in nanotubes. These molecules are obtained by rolling a graphene sheet (a single layer from a three dimensional graphite crystal) into a cylinder. By capping each end of the cylinder with half a fullerene molecule, a “fullerene derived tubule” is formed [36]. Conducting nanotubes have been observed to exhibit a zero resistance and a high critical temperature [37]. Recently, the smallest possible carbon nanotube, with a diameter corresponding to a  $C_{20}$  dodecahedron [38,39] has been synthesized. Due to the very large curvature of the nanotube walls such an atomic wire may display an array of very interesting properties.

As it emerges from the discussion above, and from the very recent date of the (few) references existing on the subject, the study of the coupling of electrons to the surface of fullerenes and of nanotubes is a subject lying at the forefront of research in solid state physics and in the construction of nanostructured materials.

### 3. Absorption and emission of photons: the colour of finite systems

It is known that the properties of finite many-particle systems do not depend so much on the nature of the constituents particles or the forces acting among them, but on the fact that these are confined in their motion by a surface and that there are many [10]. Thus, the analogies which can be carried out between the atomic nuclei and atomic aggregates like fullerenes and metal clusters [40,41], can be used profitably in the selection of these building blocks needed to produce materials displaying customer designed characteristics. In particular colours and tonalities, which reflect the photoabsorption distribution of frequencies of finite systems [42]. From these analogies it emerges that the strategies devised during the last years in

the design of nanophase materials [43], depend to a large extent on the surface of these clusters.

### 3.1. Metal clusters

A great deal of our basic insight of the world around us comes from the colours that we perceive. It is no accident that colours are used to describe emotions, and that they are an essential tool for artists to convey their feelings. An excellent example is provided by the stained glass used by Medieval architects in their cathedral windows. The architecture seems to defy gravity, whilst the warm colours of their *vitraux* produce a profoundly spiritual atmosphere when touched by the rays of the sun. Small silver and copper particles dissolved in the glass leads to the blues and the distinct ruby colours are produced by the presence of gold particles (Fig. 19). When trying to understand the “colour” of these particles, it is not enough to make reference to the optical response of either the individual atoms or bulk metal crystals. This is because we still do not know how the properties of a solid gradually evolve as atoms are brought together to form increasingly larger units. We understand reasonably well the end points of such evolution, but have still a poor knowledge of the intermediate situations. A sodium atom has a very simple absorption spectrum. It consists of essentially one line in the visible, the well-known yellow light. In quantum physics this phenomenon is well described as a one-electron transition from a quantal state, known as 3s, to an excited state, denoted by 3p. A sodium crystal, on the other hand, has a completely different spectrum. The absorption is strong in the infrared, goes through a minimum in the visible, and then rises again in the ultraviolet. The reason for this is that very low-energy photons can excite electrons from the continuum of states just below the energy of the last-occupied state (Fermi energy) to states just above the Fermi energy. The strong ultraviolet absorption is caused by interband transitions.

Suppose we chip off a small corner of a crystal, producing a microcrystal of only eight atoms. Again, the absorption spectrum changes completely. A relatively broad absorption maximum (resonance) appears in the visible (Fig. 20). This

absorption is due to a collective excitation of outer electrons called a plasmon excitation (cf. Fig. 5). It can be viewed as a collective sloshing motion of the electrons from one side of the microcrystal to the other side of it, in a similar way to tea oscillating inside a cup which we carry in our hands. It is clear that such a motion has a strong dipole moment, behaving as an antenna and thus giving rise to a strong absorption band in the visible. The absorption of light by a sodium atom is well described within the picture of independent particle motion. This picture, however, cannot describe even qualitatively the resonance phenomenon (plasmon excitation) that dominates the optical response of a eight-atom cluster. Between one atom and eight we must completely change our way of looking at the optical response of the system. As we shall see this task is eased a good deal by making use of well-established results in nuclear physics, in particular those associated with the interplay between the giant dipole resonance (plasmon in the cluster case) and the surface of the system.

### 3.2. Damping of collective motion: the case of the atomic nucleus

As already mentioned, the surface of the nucleus, similar to that of a liquid drop, can be set into vibration. This implies, according to quantum mechanics, that the nuclear surface will fluctuate also when the nucleus is in its ground state due to the zero-point motion associated with the vibrations. The dipole vibration can then be viewed as taking place in an ensemble of nuclei displaying different shapes. The absorption of gamma rays will thus have a frequency distribution reflecting the differences in radii of the shapes measured along the three axis in a coordinate system fixed to the nucleus (Fig. 21). Each of the dipole vibrations along these axis carries one-third of the strength of the dipole mode (so called energy weighted sum rule (EWSR)). Because of symmetry relations, the most important of these fluctuations for the damping process are of quadrupole type, that is shapes that look like a spheroid, a cigar or a pancake being two particular realizations of it. A simple consequence of this picture is the fact that

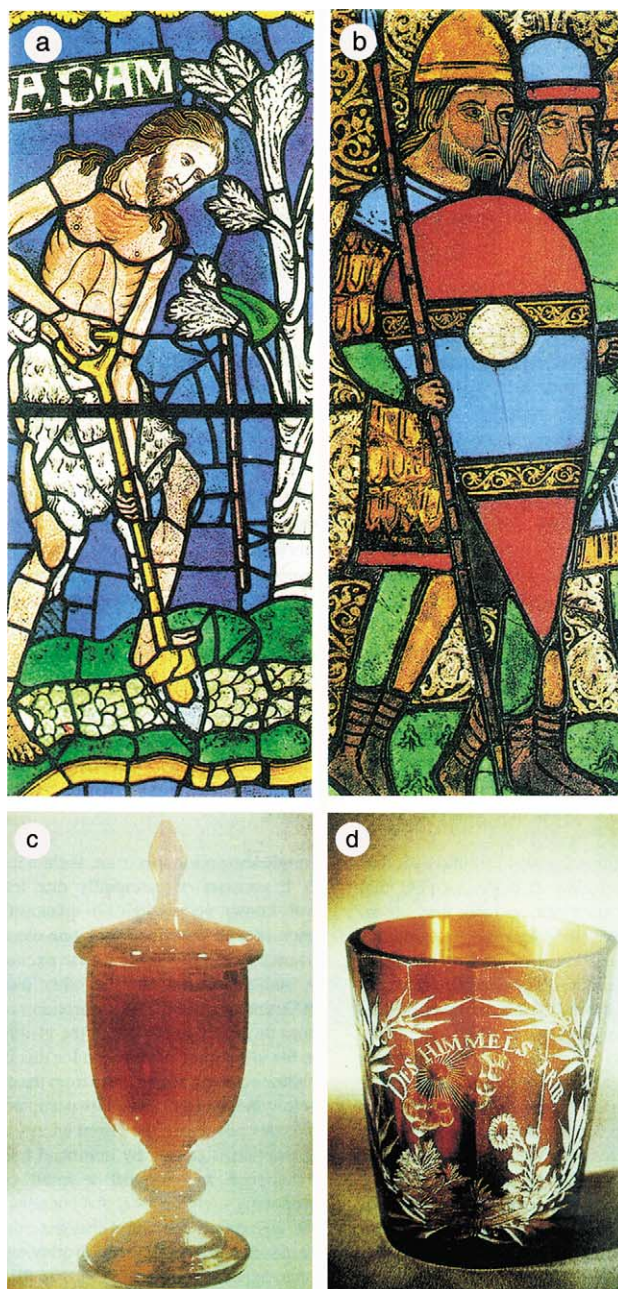


Fig. 19. (a,b) Stained glass from the Middle Ages. (a) Adam, from the great west window of Canterbury Cathedral, England (c. 1180). The blue of the background arises through the presence of small silver and copper particles. (b) Three warriors (before 1166), from the church of St Patrokli in Soest, Germany. (c) An original Bohemian glass displaying its warm ruby colour arising from the presence of gold particles. (d) A glass produced c. 1700 in Berlin, where a glass-blower of this city reinvented the recipe of dissolving gold particles in glass.

in the case of nuclei displaying static prolate deformations one expects two peaks, one at lower

energy associated with oscillations along the symmetry axis, and another at higher energy

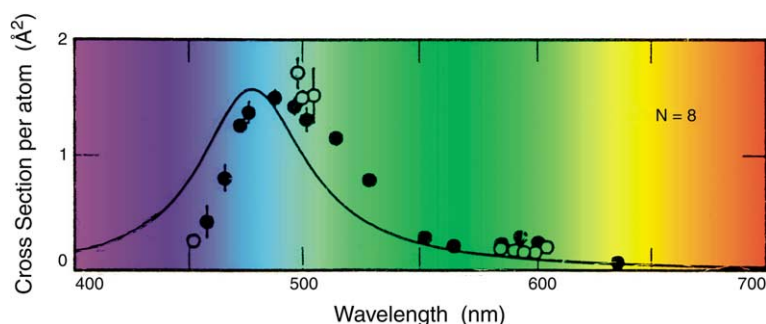


Fig. 20. Photoabsorption strength function associated with a cluster containing eight atoms of Na, as a function of the wavelength [44]. The frequency of the vibration of electrons against the ions (cf. Fig. 5) falls into the visible region of the spectrum, as indicated by the colours. The continuous curve corresponds to a theoretical calculation [45].

associated with vibrations in a plane perpendicular to the symmetry axis. Along the symmetry axis there is only one possible dipole mode, while there are two directions perpendicular to each other for dipolar vibrations in the plane perpendicular to the symmetry axis. Consequently, the lower peak carries one-third of the total intensity, while the higher peak carries two-thirds. Clear evidence for this effect has been observed (Fig. 22).

Nuclei cannot only become deformed, the ratio between the smallest and the largest radius being 1:1.2, they can also become superdeformed, when this ratio is 1:2. These are the largest deformations a nucleus can sustain without fissioning (Fig. 8), and it was a *tour de force* to detect the quadrupole transitions de-exciting systems rotating with such a shape [46]. With a new generation of  $\gamma$ -ray detectors, like EUROBALL [3], the brainchild of six European countries (Italy, France, Denmark, Germany, Sweden, England), which are able to cover, at a price tag of approximately 30 million dollars, a conspicuous fraction of the full solid angle, it has been possible to make even a more remarkable *tour de force*, namely that of measuring the  $\gamma$ -decay of a giant dipole resonance in coincidence with the  $\gamma$ -decay of the members of the superdeformed rotational band (Fig. 23). Thereby allowing the determination of the effect superdeformation of the nuclear surface has on the dipole vibration of the system. The results which have only recently become available [47], but which were predicted more than 15 years ago [48], are spectacular, implying a splitting between the

energy associated with vibrations along the symmetry axis and in the plane perpendicular to it of about of 10 MeV as compared to a centroid energy of the order of 15 MeV. This result demonstrates the fact that large deformations make the atomic nucleus extremely polarizable [49].

### 3.2.1. Damping of plasmons: an analogy

Turning now to metal clusters, the calculated frequency of the photoabsorption peak (plasmon) turns out to be proportional to the frequency of the plasmons in bulk matter, a result that agrees well with the experimental findings. Consequently, it is largely independent of the dimensions of the cluster. This result, which can be traced back to the long range of the Coulomb force, is very different from that obtained in the nuclear case, where the centroid of the resonance was found to be inversely proportional to the dimension of the system. In spite of this difference, the method used in the nuclear case for calculating the spreading width of the vibrations can still be applied here [45]. One can make use of the fact that the back and forth sloshing of the electrons in a quadrupole-deformed cluster is associated with electric fields, and thus depolarizability factors, which differ greatly depending on whether the dipole vibration takes place along the largest or the smallest radius (Fig. 21, bottom).

A remarkable example of the central role played by the surface of the cluster in the damping of the plasmon oscillation is provided by the optical response of deformed clusters. From microscopic



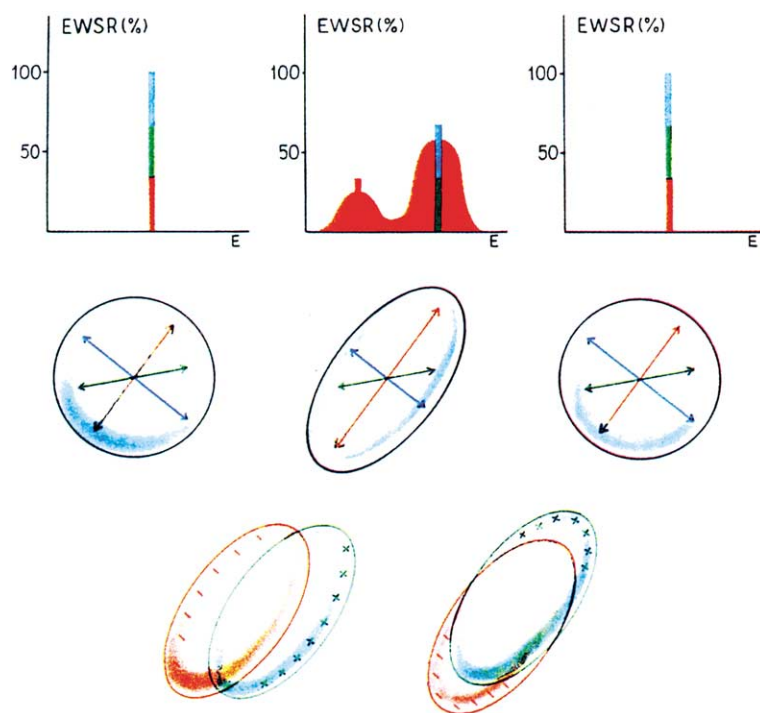


Fig. 21. Schematic representation of the mechanism that is at the basis for the damping of the giant dipole resonance in both atomic nuclei and metal clusters [10,49]. A finite system can vibrate as an antenna along three directions in space perpendicular to each other. The frequency of these vibrations in a nucleus are identical for a spherical configuration, in keeping with the fact that the frequency of the giant dipole resonance is inversely proportional to the radius of the system. For a quadrupole deformed (axially symmetric) nucleus, the single line splits into two, as there are two radii defining the system, one along the symmetry axis and one perpendicular to it. These situations are illustrated (top) where the EWSR of each of the contributions to the dipole vibration is shown as a function of excitation energy. Immediately below a schematic representation of the nuclear shapes and associated dipole vibrations is given. Because the nuclear shapes fluctuate as a function of time, the system will cover in a continuous fashion other deformations besides those explicitly shown, leading not only to a splitting of the strength, but also to a resonant peak with a distinct line shape (see middle top figure). (bottom) The dipole vibrations of electrons against the positive ions in a deformed metal cluster are shown. The positive and negative signs represent the excess of ions and of electrons respectively associated with the dynamical situation of departures from equilibrium during the vibration. The associated dipole fields are very different according to whether the vibration takes place along the symmetry axis or perpendicular to it.

considerations associated with the orbitals occupied by the electrons in the cluster ground state, sodium clusters containing 12 atoms are expected to display triaxial shapes. Consequently, one would expect a three peak structure for the associated surface plasmon. Experiments [44] have confirmed these expectations (Fig. 24). Microscopic calculations can explain these results in terms of dipolar vibrations along the  $x$ -,  $y$ - and  $z$ -axis of a coordinate system fixed to the cluster [50]. Although there are a number of nuclei that are also predicted to display triaxial equilibrium de-

formations, no giant dipole resonance with more than two peaks has been observed in the nuclear case. This is because the relatively large fluctuations and smaller static deformations displayed by the nuclear surface as compared with the cluster surface lead, in the nuclear case, to widths for each individual lines that blur the three peak structure. Summing up, the frequencies at which both atomic nuclei as well as metallic clusters absorb electromagnetic radiation, are strongly influenced by the shape of the surface of the system and by the spill-out of fermions from it.

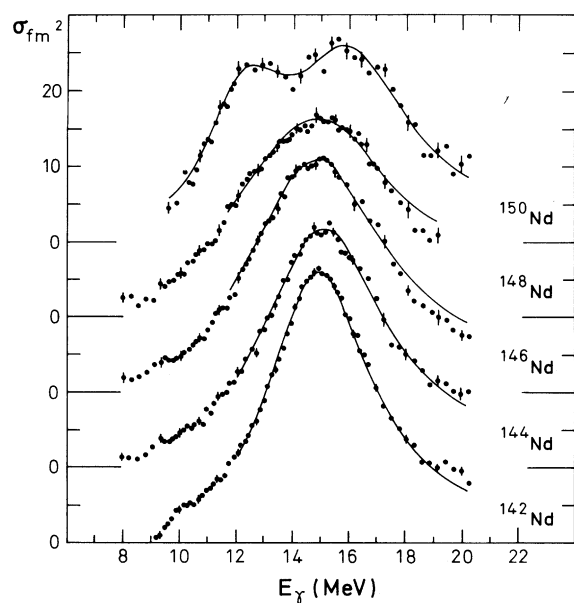


Fig. 22. Photoabsorption cross section for even isotopes of neodymium as a function of the energy of the absorbed photon (excitation energy of the system). While  $^{142}\text{Nd}$  is spherical,  $^{150}\text{Nd}$  is well deformed, the transition between spherical and deformed shapes been evidenced by a broadening of the resonance.

### 3.3. Atomic wires

Metals tend to be highly absorbing at long wavelengths (visible and infrared). Nanometre wires are thus expected to display this same property. Consequently, from the arguments developed in the previous sections, these wires are likely to be found among finite atomic aggregates displaying strong deformation and particle spill out. Among the systems satisfying these requirements, single-wall nanotubes and linear carbon chains seem to be particularly promising. In fact, theoretical [40,51,52] and experimental [53] studies have shown that they behave as metallic needles when subject to an electromagnetic field (cf. Fig. 25(c)). Consistent with this result, it has also been calculated [51] that, under standard bias conditions, i.e. subject to a moderate potential difference, linear chains made out of few carbon atoms are prolific emitters of electrons, the associated currents versus voltage curves displaying a

behaviour typical of metallic systems (Fig. 25(a) and (b)). These results are consistent with the experimental findings of Ref. [54] where it is reported that: “field emission of electrons from individually mounted carbon nanotubes has been found to be dramatically enhanced when the nanotube tips are opened by laser evaporation or oxidative etching. Emission currents of 0.1–1  $\mu\text{A}$  were readily obtained at room temperature, with a bias potential of 80 V. The emitting structures are concluded to be linear chains of carbon atoms  $\text{C}_n$  ( $n = 10\text{--}100$ ), pulled out from the graphene wall layers of the nanotube by the force of the field, in a process that resembles unravelling the sleeve of a sweater”. In other words, a “wire” (connected to an electron reservoir) made out of a few carbon atoms and of length of the order of a nanometre (Fig. 26), i.e. one billionth of a metre emits, under the influence of a modest electric field, a current as intense as a microampere.

Nanotubes and linear carbon chains are thus likely to constitute, among other things, the ultimate atomic-scale quantum wires and electron guns to make connections in nano-circuits and to produce extremely flat television screens [55] (Fig. 27).

It is interesting to note that while a chain of eight atoms is expected [51] to be able to emit, connected to an electron reservoir, currents of the order of microamperes, a linear chain of seven atoms is predicted to emit, under the same bias conditions, currents which are two orders of magnitude weaker. Making use of an analogy, it is as if by making a piece of wire just slightly shorter, one changed its electric properties completely. Within this contest it is worth remembering that Nobel Laureate Richard P. Feynman addressing the Annual Meeting of the American Physical Society on 29 December 1959 said: “...When we get to the very, very small world—say circuits of seven atoms—we have a lot of new things that would happen that represent completely new opportunities for design. Atoms on a small scale behave like nothing else on a large scale, for they satisfy the laws of quantum mechanics” [56]. In fact, it is precisely quantum mechanics which rules that  $\text{C}_7$  is a much more stable system than  $\text{C}_8$ , and con-

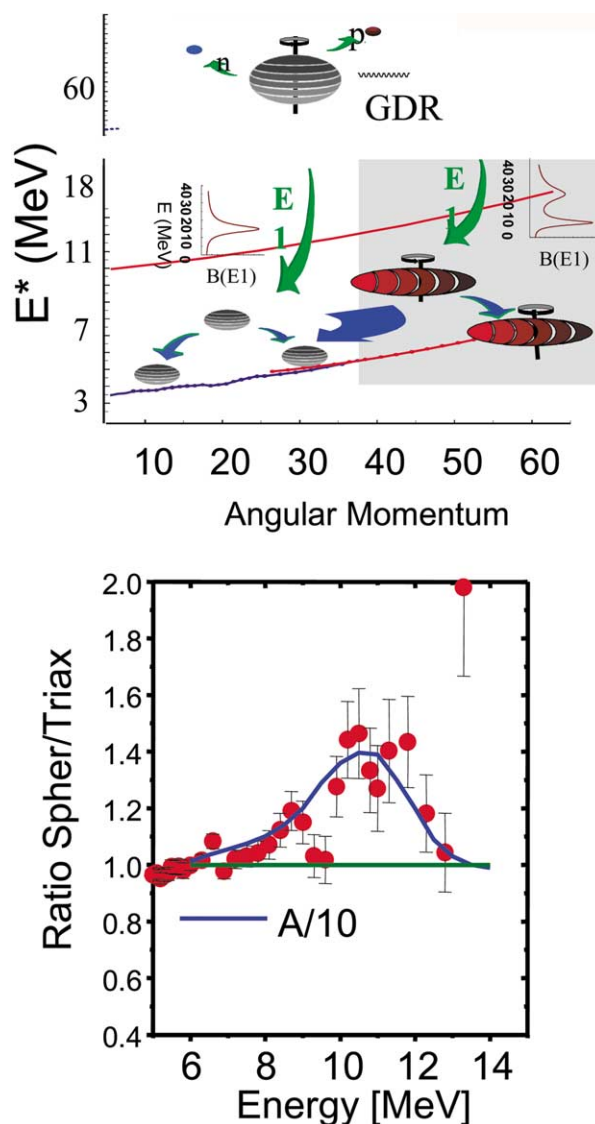


Fig. 23. Schematic representation of the formation and  $\gamma$ -decay of a superdeformed compound nucleus (upper part). In the bottom part we show the low-energy strength function associated with the decay of the giant dipole resonance of the nucleus  $^{143}\text{Eu}$  in its superdeformed configuration (the ratio between the largest and the smallest radii being 2:1). The analysis of the data (blue curve going through the experimental points (red dots with error bars) above the background given by the green horizontal line) was carried out making use of a density of levels corresponding to a (density parameter) value of  $A/10$ , where  $A$  is the mass number of the nucleus. The measurements were carried out by recording hard  $\gamma$ -rays i.e. photons of energy in the range of energy from 5 to 20 MeV associated with the decay of the giant dipole resonance in coincidence with  $\gamma$ -rays corresponding to transitions connecting members of the superdeformed rotational band of  $^{143}\text{Eu}$ . This was done to ensure that the dipole vibrations measured are based on the superdeformed minimum of the system.

sequently it is much more difficult to extract an electron out of  $C_7$  than of  $C_8$ .

While  $C_7$  may not be a too good a field emitter, it is interesting to note that the electromagnetic

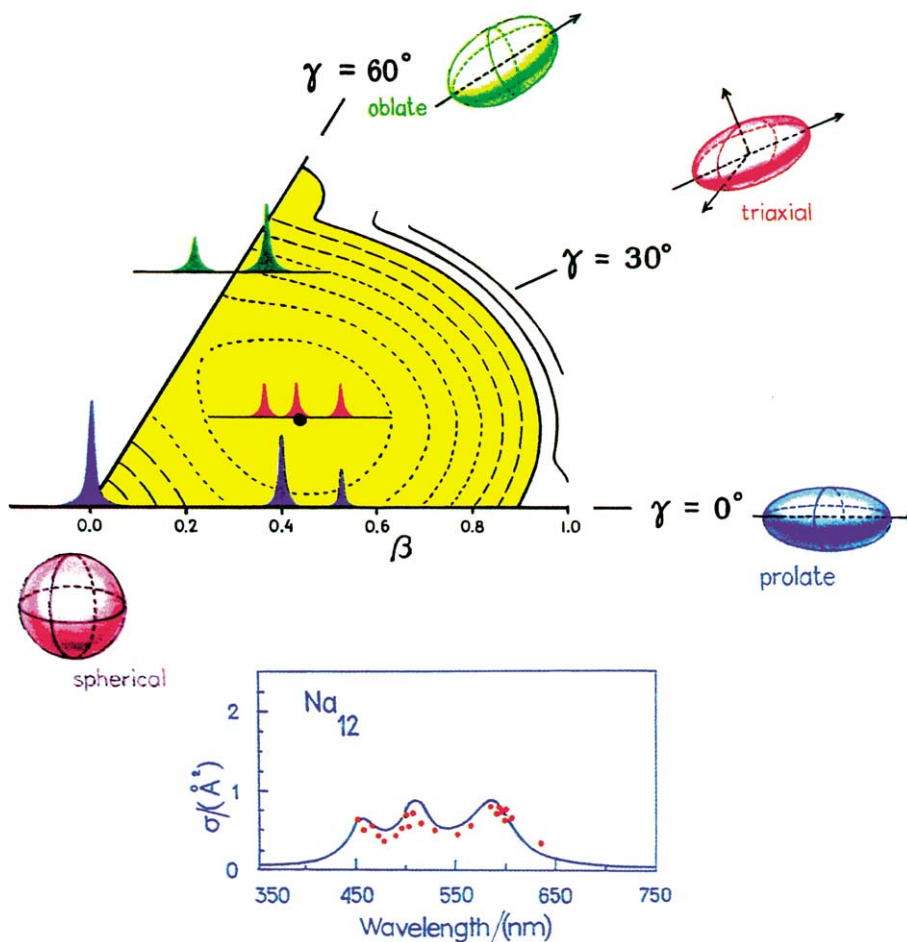


Fig. 24. The independent particle model of metal clusters predicts that the aggregate  $\text{Na}_{12}$  containing 12 atoms of sodium is strongly deformed, displaying three different radii along the principal axis. The potential energy surface of this cluster in the plane of the deformation parameters  $\beta$  (characterizing the quadrupole moment of the cluster) and  $\gamma$  (characterizing the departure from axial symmetry) is shown in the top part of the figure. Also shown are the shapes of the photoabsorption strength function (cf. also Fig. 21) for the different shapes of the system: spherical (one peak), axially symmetric oblate or prolate shapes (two peaks), triaxial (three peaks). Because the cluster is at non-zero temperature, it can be viewed as an ensemble of systems with different shapes, with probabilities fixed by the corresponding Boltzmann factors [49]. Calculations of the line-shape of the surface plasmon taking these effects into account have been carried out in Ref. [50]. They are shown (blue curve) in comparison with the data from [44] (red dots) in the lower part of the figure.

response of the anion  $\text{C}_7^-$  (among others) has important astrophysical implications, as we shall see below.

### 3.4. Diffuse interstellar bands

Just as dust particles in the earth atmosphere produce a red sunset, so starlight is reddened as

it passes through clouds of interstellar dust. The visible-ultraviolet spectrum from distant stars is like the spectrum of the sun, our nearby star, crossed by a series of narrow, dark lines. But in the spectrum of distant stars, aside from these lines, which are associated with the absorption of light by atoms present in the outer layers of the sun, there are others that are much broader (or more

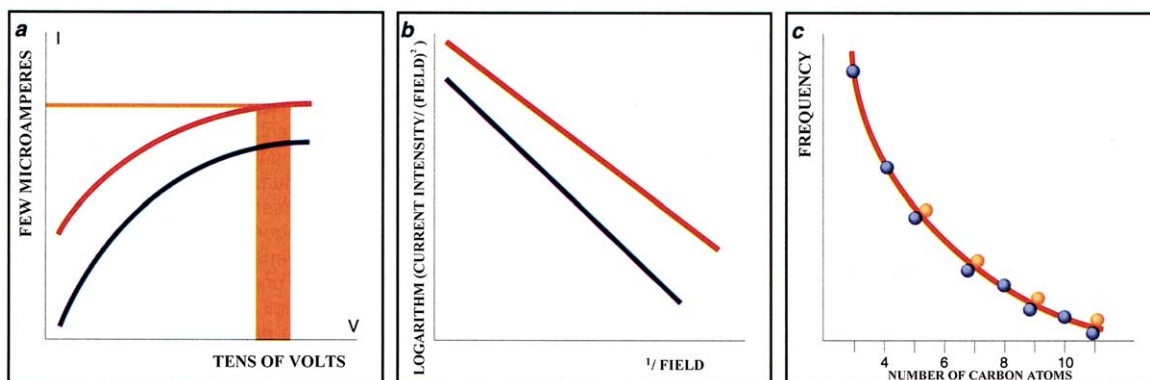


Fig. 25. (a) Applying a potential difference to linear carbon chains made out of seven (blue continuous curve) and of eight (red continuous curve) atoms leads, according to quantal calculations [51], to currents (known as field emission currents), with intensities differing by two orders of magnitudes. Chains with few and even number of carbon atoms can thus be very efficient atomic electron guns. (b) Plotting the logarithm of the current intensity  $I$  displayed on the ordinate of (a) divided by the square of the applied electric field as a function of the inverse of the field, corresponding to the abscissa of (a), a linear dependence is observed. Quantum mechanics predicts such a behaviour in the case of field emission from metallic particles. (c) Quantal calculations [51,52] predict that when a beam of photons, whose polarization plane contains the symmetry axis of the linear carbon chain  $C_n$  studied ( $n = 3, 4, \dots, 11$ ), is shone on the chain, the system absorbs energy at essentially a single frequency (blue dots). This frequency is quite close to that experimentally [53] observed (orange dots). The quantal results are well reproduced by a classical expression which depends on the ratio of the shortest to the longest radius of the chain, and which describes the behaviour of the macroscopic elongated metallic particles, of similar (scaled) shape as the linear carbon chain studied (red curve).

diffuse). For this reason they are referred to as bands rather than lines. The quest for the origin of these diffuse interstellar bands (DIB), dubbed by Harry Kroto “the last great problem in astronomy”, is closely related to the presence of carbon in the Universe [57]. In particular, as it has been argued since 1977, of linear carbon chains [58–62]. One knows today that the answer to the origin of DIB is more articulated than that proposed in Ref. [58] (cf. e.g. Ref. [59] and Fig. 28). In any case, a number of optical gas phase electronic transitions (plasmons) of linear carbon chains anions (i.e. charged chains), recently observed in the laboratory [65], have been found to coincide with some of the DIB [63] (Fig. 28). In this connection, one can mention that first principal calculations of the spectrum of linear neutral carbon chains [64] as well as experimental data in inert gas matrices [53] (Fig. 25c), indicate also the coincidence of few of the corresponding lines with DIB. Because the spectrum of a quantal system is as revealing of its identity as fingerprints are of individuals, the findings of Ref. [63] reopens the case of linear carbon chains in connection to the question of DIB.

#### 4. Resume and outlook

It is tempting to ask whether there is any fundamental reason or unifying concept, that makes it simple to understand and, in hindsight, “predict” the paramount role the surface of finite systems plays in determining their properties, and the properties of bulk materials they can form. The answer to this question is to be found in the principles lying at the foundations of quantum mechanics, the theoretical framework of the very small, where the symmetry concepts associated with the isotropy of space and time play a primary role [67]. The fact that space is isotropic implies that the quantal description of a system, in particular of a finite system, will not depend on its orientation. Thus, when a little nucleus, suspended in isotropic space and isolated from anything else deforms spontaneously in order to lower its energy, it has two choices for respecting the rules of the game: either to make the deformation static and then rotate collectively, averaging in this way the orientation of the system (collective rotations), or to make the deformation dynamic and vibrate

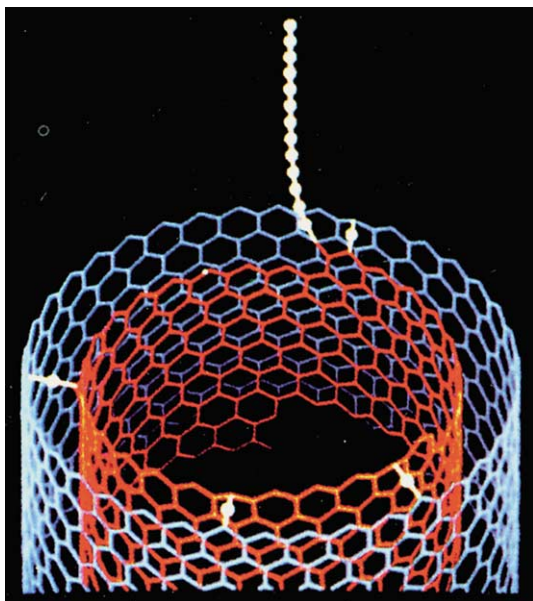


Fig. 26. Model of the tip of a multiwall nanotube (red and blue layers) showing a single  $C_n$  “atomic wire” extending out from the inner layer, held taut and straight by the electric field (after Ref. [54]). It is still an open question what the energy difference between the open-ended and the closed configurations of the multi wall nanotubes (MWN) used in Ref. [54] is under the biased applied. It has been shown that this difference decreases with increasing field [76], although it is unlikely it may be sufficient to lower the open end energy below that associated with the capped structure. How the situation is modified in MWN is an open question.

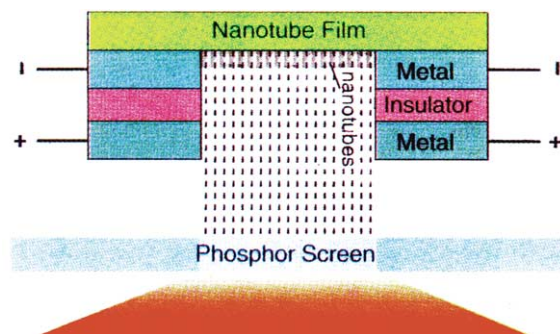


Fig. 27. Field emission is defined as the emission of electrons from the surface of a condensed phase into another phase, usually vacuum, under the action of an electrostatic field. The phenomenon consists in the tunneling of electrons through a potential barrier at the surface, in this case, of nanotubes (in the case of Fig. 25 of linear carbon chains). In the figure, a schematic diagram of the field emitting set up based on nanotubes is displayed [55]. Under a difference of potential it shoots electrons (—) at a phosphor display, triggering light emission.

(collective surface vibrations). Consequently, the phenomenon of spontaneous symmetry breaking makes the nuclear surface a source of collective motion. The motion of the nucleons will reflect, through the coupling of particles and vibrations, this privileged role of the nuclear surface. Because all the degrees of freedom determining the nuclear structure are exhausted by the degrees of freedom

Fig. 28. In 150 B.C. the Greek astronomer Hipparchus grouped the sky's stars into six brightness categories called magnitudes, first magnitudes representing the brightest stars he saw, sixth the faintest. The apparent magnitude ( $m$ ) of a star—the magnitude as seen by Hipparchus and by us—depends on the star's real luminosity (i.e., on the amount of energy it radiates on watts) and on its distance. A star may seem bright to us either because it is nearby (even though faint) or because, though far away, it is very luminous. If we know the star's distance ( $d$ ), we can find its luminosity from its apparent brightness. In astronomy, luminosity is expressed by a star's absolute magnitude ( $M$ ), the value the apparent magnitude would have at a standard distance of 10 parsecs, that is, of 32.6 light years (the light year is the distance light travels in vacuum in a year). The two kinds of magnitude are related by the magnitude equation  $M = m + 5 - 5 \log d$ , where  $d$  is in parsecs. To apply the method of spectroscopic distances we must correct the apparent magnitude of a star for the dimming by the interstellar dust. This means knowing the degree of extinction ( $A$ ), the magnitude by which the apparent visual magnitude must be brightened (i.e., the amount by which its value must be decreased) before it is entered into the magnitude equation. One can find  $A$  because it scales with the degree of reddening. (a) The extinction function—the dependence of interstellar extinction to wavelength  $\lambda$ —has a rough  $\lambda^{-1}$  dependence in the optical and goes to zero at long wavelength (allowing correlated far-infrared and radio waves to penetrate interstellar space with penache). In the ultraviolet, interstellar space becomes remarkably opaque; the 2000 Å bumps have been found to be correlated with the laboratory spectrum of matrix-isolated nanometer-sized carbon particles (after Ref. [66]). (b) Two typical structures of carbon particles taken with high-resolution transmission electron microscope: (left) carbon particle with randomly oriented basic structural units, (right) onion-type carbon particle with several condensation seeds (cf. Ref. [56]). Theoretical calculations indicate the multishell fullerenes (carbon onions) to be the likely candidates for the 2200 Å bumps. (c) DIB observed as broad depressions in stellar spectra are seen from the ultraviolet through the near-infrared (after Ref. [66]). (d) Gas-phase electronic transitions of  $C_7^-$  (charged linear carbon chain containing seven atoms of carbonium) recorded in the laboratory [62] (upper trace). The bottom trace shows a Gaussian fit to the tabulated DIB. Those labeled with an asterisk coincide with the measured bands of  $C_7^-$  above.

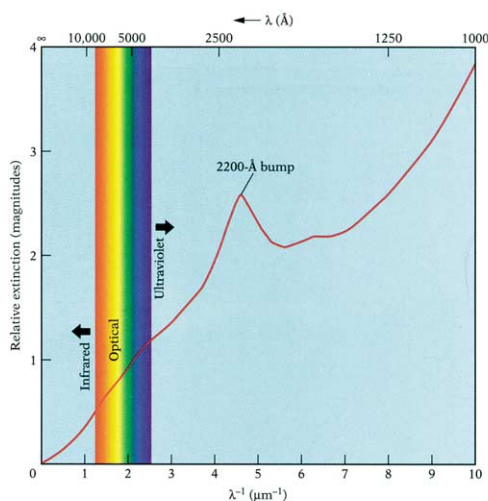


of protons and neutrons, essentially all (low-energy) nuclear properties will depend on the surface of the system. This is also true for other physical systems such as metal clusters, fullerenes, nanotubes and linear carbon chains in particular, and finite many-body systems in general. Also for the materials constructed out of these systems.

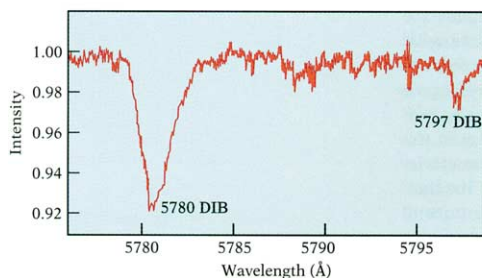
It is interesting to think that the riddle connected with the surface of finite systems touches, through the phenomenon of spontaneous symme-

try breaking, also on fundamental physical questions like the existence of Goldstone bosons [68–70]. That is, zero-mass particles like the photon, the carriers of the Coulomb force, and the pion, one of the carriers of the strong force. In the case of the nucleus, Goldstone bosons are intimately connected with zero-frequency vibrations and associated rotations [11,71,72]. The Higgs boson [73], the missing building block of the unified theory of elementary particles, the quest of which

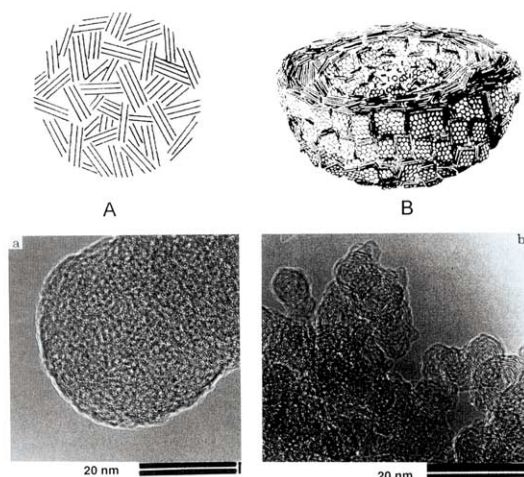
(a)



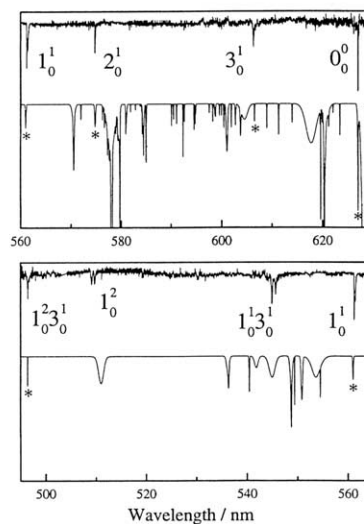
(c)



(b)



(d)



will be the main research activity of the largest accelerator ever built (Large Hadron Collider (LHC) of CERN in Switzerland), is a consequence of a “frustrated” phenomenon of spontaneous symmetry breaking as is the most mundane plasmon (electron vibrations) in condensed matter [74].

Once on the subject, one could ask the even deeper question: “why spontaneous symmetry breaking at all?”. While this is the most basic and challenging question emerging in trying to understand the role played by the surface of finite systems in determining their properties, it lies outside the scope of the present paper. To the interested reader one can suggest contemplating the connection existing between quantal and classical mechanics, remembering the fact that the solutions of Newtonian mechanics do not have to respect particular symmetries as quantal solutions do. In particular the rotational invariance of empty space as demonstrated by the fact that our reader is able to find out whether the page he or she is reading is upside down or not.

A unified understanding of the surface of finite systems, of which the atomic nucleus can be viewed as a paradigm is expected to shed light, at the fundamental level, on the strategy used by nature in creating cosmic patterns, from exotic nuclei to neutron stars. It is also expected to shed light on man made nanometer materials, materials which have changed and will continue to change our daily life, from the stained glasses of medieval cathedrals to science fiction-like electron guns.

## Acknowledgements

I wish to thank E. Ormand and E. Vigezzi for carefully reading the manuscript. The technical help of F. Marini is gratefully acknowledged.

## References

- [1] F. Dyson, *Disturbing the Universe*, Harper and Row, New York, 1974.
- [2] M.G. Mayer, J.H. Jensen, *Elementary Theory of Nuclear Shell Structure*, Wiley, New York, 1955.
- [3] J. Simpson, EUROBALL: present status and outlook, *Heavy Ion Phys.* 6 (1997) 253.
- [4] S. Weinberg, *The First Three Minutes*, Bantam, New York, 1977.
- [5] C. Mahaux, P.F. Bortignon, R.A. Broglia, C.H. Dasso, Dynamics of the shell model, *Phys. Rep.* 120 (1985) 1.
- [6] A.L. Fetter, J.D. Walecka, *Quantum Theory of Many-Particle Systems*, McGraw-Hill, New York, 1971.
- [7] N. Bohr, Neutron capture and nuclear constitution, *Nature* 137 (1936) 344.
- [8] P. Donati, P. Pizzochero, P.F. Bortignon, R.A. Broglia, Temperature dependence of the nucleon effective mass and the physics of stellar collapse, *Phys. Rev. Lett.* 72 (1994) 2835.
- [9] Scientific opportunities with fast fragmentation beams from RIA, National Superconduction Sincrotron Laboratory, Michigan State University, March 2000, p. 43.
- [10] G.F. Bertsch, R.A. Broglia, *Oscillation in Finite Quantal Systems*, Cambridge University Press, Cambridge, 1994.
- [11] A. Bohr, B.R. Mottelson, *Nuclear Structure*, Vols. I–II, Addison-Wesley, New York, 1969, 1975.
- [12] A. Bohr, *Rotational Motion in Nuclei*, Le Prix Nobel en 1975, Norstedts Tryckeri, Stockholm, 1976, p. 56.
- [13] B.R. Mottelson, *Elementary Modes of Excitation in Nuclei*, Le Prix Nobel en 1975, Norstedts Tryckeri, Stockholm, 1976, p. 80.
- [14] J. Rainwater, *Background for the Spheroidal Nuclear Model Proposal*, Le Prix Nobel en 1975, Norstedts Tryckeri, Stockholm, 1976, p. 102.
- [15] J.R. Schrieffer, *Theory of Superconductivity*, Benjamin, New York, 1964.
- [16] P.W. Anderson, *The Theory of Superconductivity in high  $T_c$ -cuprates*, Princeton University Press, Princeton, 1997.
- [17] D.M. Lee, The extraordinary phase of liquid  $^3\text{He}$ , Nobel Lecture, *Rev. Mod. Phys.* (1998);  
D.D. Osheroff, Superfluidity in  $^3\text{He}$ : discovery and understanding, Nobel Lecture, *Rev. Mod. Phys.* (1998);  
R.C. Richardson, The Pomeranchuk effect, Nobel Lecture, *Rev. Mod. Phys.* (1998);  
B. De Marco, D.S. Jin, *Science* 285 (1999) 1703;  
B. De Marco, D.S. Jin, *News, Science* 285 (1999) 1646.
- [18] F. Barranco, R.A. Broglia, G. Gori, E. Vigezzi, P.F. Bortignon, J. Terasaki, Surface vibrations and the pairing interaction in nuclei, *Phys. Rev. Lett.* 83 (2000) 2147.
- [19] S. Austin, G.F. Bertsch, Halo nuclei, *Sci. Am.* 272 (1995) 62.
- [20] M. Zinser et al., Invariant mass-spectroscopy of  $^{10}\text{Li}$  and  $^{11}\text{Li}$ , *Nucl. Phys. A* 619 (1997) 157.
- [21] F. Barranco, R.A. Broglia, G. Coló, E. Vigezzi, The halo of the exotic nucleus  $^{11}\text{Li}$ : a single Cooper pair, *Europhys. J. A* 11 (2001) 385.
- [22] *Radioactive Nuclear Beam Facilities*, NuPECC Report, April 2000.
- [23] D. Pines, M.A. Alpar, in: D. Pines, R. Tamagaki, S. Tsuruta (Eds.), *The Structure and Evolution of Neutron Stars*, Addison-Wesley, New York, 1992.



- [24] A. Alpar, Pulsars, glitches and superfluids, *Phys. World* 11 (1998) 25.
- [25] P.M. Pizzochero, L. Viverit, R.A. Broglia, Vortex-nucleus and pinning forces in neutron stars, *Phys. Rev. Lett.* 79 (1997) 3347.
- [26] A. Hewish, Pulsars and high density physics, Nobel Lecture, *Rev. Mod. Phys.* 47 (1975) 567.
- [27] P. Anderson, M.A. Alper, D. Pines, J. Shaham, The rheology of neutron stars. Vortex-line pinning in the crust super-fluid, *Philos. Mag.* 45 (1982) 227.
- [28] R.F. Curl, Dawn of the fullerenes: experiment and conjecture, Nobel Lecture, *Rev. Mod. Phys.* 69 (1997) 691; H. Kroto, Symmetry, space, stars and  $C_{60}$ , Nobel Lecture, *Rev. Mod. Phys.* 69 (1997) 703; R.E. Smalley, Discovering the fullerenes, Nobel Lecture, *Rev. Mod. Phys.* 69 (1997) 723.
- [29] O. Gunnarsson, Superconductivity in fullerides, *Rev. Mod. Phys.* 69 (1997) 575.
- [30] J.H. Schön, Ch. Kloc, B. Batlogg, High-temperature superconductivity in lattice-expanded  $C_{60}$ , *Nature* 293 (2001) 2432.
- [31] A. Devos, M. Lanoo, Electron–phonon coupling for aromatic molecular crystals: possible consequences for their superconductivity, *Phys. Rev. B* 58 (1998) 8236; M. Lanoo, G.A. Baraff, M. Schlüter, D. Tomanek, Jahn–Teller effect for the negatively charged  $C_{60}$  molecule: analogy with the silicon vacancy, *Phys. Rev. B* 44 (1991) 12106; K. Yabana, G.F. Bertsch, Comment on “Jahn–Teller effect for the negatively charged  $C_{60}$  molecule: Analogy with the silicon vacancy”, *Phys. Rev. B* 46 (1992) 14263.
- [32] M. Coté, J.L. Grossman, M.L. Cohen, S. Louie, Electron–phonon interactions in solid  $C_{36}$ , *Phys. Rev. Lett.* 81 (1998) 679.
- [33] N. Breda, R.A. Broglia, G. Coló, G. Onida, D. Provasi, E. Vigezzi,  $C_{28}$ : a possible room temperature organic superconductor, *Phys. Rev. B* 62 (2000) 130.
- [34] H. Prinzbach, P. Landenberger, F. Wahl, J. Worth, L. Scott, M. Gelmont, D. Olevano, B. von Issendorf, Gas-phase production and photoelectron spectroscopy of the smallest fullerene, *Nature* 407 (2000) 60.
- [35] A. Lanzara et al., Evidence for ubiquitous strong electron–phonon coupling in high temperature superconductors, *Nature* 412 (2001) 510.
- [36] R. Saito, G. Dresselhaus, M.S. Dresselhaus, *Physical Properties of Carbon Nanotubes*, Imperial College Press, London, 1998.
- [37] A. Yu et al., Supercurrents through single-walled carbon nanotubes, *Science* 284 (1999) 1508.
- [38] L.-C. Qin, X. Zhao, K. Hirahara, Y. Miyamoto, Y. Ando, S. Iijima, The smallest carbon nanotube, *Nature* 408 (2000) 50.
- [39] N. Wang, Z.K. Tang, G.D. Li, J.S. Chen, Single-Walled 4 Å carbon nanotubes arrays, *Nature* 408 (2000) 50.
- [40] R.A. Broglia, F. Alasia, P. Arcagni, G. Coló, F. Ghielmetti, C. Mikani, H.E. Roman, Softening the long-wave-length electromagnetic response of finite quantal systems, *Z. Phys. D* 40 (1997) 240.
- [41] W. de Heer, The physics of simple metal clusters: experimental aspects and simple models, *Rev. Mod. Phys.* 65 (1993) 611; M. Brack, The physics of simple metal clusters: self-consistent jellium model and semiclassical approaches, *Rev. Mod. Phys.* 65 (1993) 677.
- [42] G.F. Bertsch, Vibrations of the atomic nucleus, *Sci. Am.* 248 (1983) 40.
- [43] R.W. Siegel, Creating nanophase materials, *Sci. Am.* 275 (1996) 42.
- [44] K. Selby, M. Vollmer, J. Masui, V. Kresin, W.A. de Heer, W.D. Knight, Surface plasma resonances in free metal clusters, *Phys. Rev. B* 40 (1989) 5417.
- [45] J.M. Pacheco, R.A. Broglia, Effect of surface fluctuations in the line shape of plasma resonances in small metal clusters, *Phys. Rev. Lett.* 62 (1989) 1400.
- [46] P.J. Nolan, P.J. Twin, Superdeformed shapes at high angular momentum, *Ann. Rev. Nucl. Part. Sci.* 38 (1988) 533–562.
- [47] A. Bracco, F. Camera, S. Leoni, B. Million, A. Maj, M. Kmiecik, The giant dipole resonance in superdeformed nuclei and the feeding of superdeformed bands, *Nucl. Phys. A* 687 (2001) 237c–244c.
- [48] M. Diebel, M. Gallardo, T. Døssing, R.A. Broglia, Damping of the giant dipole resonance in hot, strongly rotating nuclei, *Nucl. Phys. A* 443 (1985) 415.
- [49] P.F. Bortignon, A. Bracco, R.A. Broglia, *Giant Resonances: Nuclear Structure at Finite Temperature*, Harwood Academic Publishers, New York, 1998.
- [50] M. Bernath, C. Yannouleas, R.A. Broglia, Deformation effects in the optical response of small metal clusters, *Phys. Lett. A* 156 (1991) 307–312.
- [51] A. Lorenzoni, H.E. Roman, F. Alasia, R.A. Broglia, High-current field emission from an atomic quantum wire, *Chem. Phys. Lett.* 276 (1997) 237.
- [52] K. Yabana, G.F. Bertsch, Optical response of small carbon clusters, *Z. Phys. D* 42 (1997) 219.
- [53] D. Forney, P. Freivogel, M. Grutter, J.P. Maier, Electronic absorption spectra of linear carbon chains in neon matrices. IV.  $C_{2n+1}$  ( $n = 2–7$ ), *J. Chem. Phys.* 104 (1996) 4954.
- [54] A.G. Rinzler, J.H. Hafner, P. Nicolaev, L. Lou, S.G. Kim, D. Tomanek, P. Nordlander, D.T. Colbert, R.E. Smalley, Unraveling nanotubes: field emission from an atomic wire, *Science* 269 (1995) 1550.
- [55] W. de Heer, A. Chatelain, D. Ugarte, A carbon nanotube field-emission electron source, *Science* 270 (1996) 1174.
- [56] R.P. Feynman, There is a lot of space at the bottom, *The Caltech Alumni Magazine* (February 22, 1960); reprinted *IEEE J. MEMS* 1 (1992) 60.
- [57] Th. Henning, F. Salama, Carbon in the Universe, *Science* 282 (1998) 2204.
- [58] A.E. Douglas, Origin of diffuse interstellar lines, *Nature* 269 (1977) 130.

- [59] P. Thaddeus, C.A. Gottlieb, R. Mollaghababa, J.M. Urtileh, Free carbenes in the instellar gas, *J. Chem. Soc. Faraday Trans.* 89 (1993) 2125.
- [60] J. Fulara, D. Lessen, P. Freivogel, J.P. Maier, Laboratory evidence for highly unsaturated hydrocarbons as carriers of some of the diffuse interstellar bands, *Nature* 366 (1993) 439.
- [61] D. Forney, M. Grutter, P. Freivogel, J.P. Maier, Electronic absorption spectra of carbon chain anions  $C_{2n+1}^-$  ( $n = 2-5$ ) in neon matrices, *J. Chem. Phys. A* 101 (1997) 5292.
- [62] P. Freivogel, M. Grutter, D. Forney, J.P. Maier, Electronic absorption spectra of carbon chain anions  $C_{2n}^-$  ( $n = 4-7$ ) in neon matrices, *J. Chem. Phys.* 107 (1997) 22; P. Freivogel, M. Grutter, D. Forney, J.P. Maier, Electronic absorption spectra of  $C_4^-$  and  $C_6^-$  chains in neon matrices, *J. Chem. Phys.* 107 (1997) 4468.
- [63] M. Tultj, D.A. Kirkwood, M. Pachkov, J.P. Maier, Gas-phase electronic transitions of carbon chain anions coinciding with diffuse interstellar bands, *Astrophys. J.* 506 (1998) L69.
- [64] M. Bianchetti, P.F. Buonsante, F. Ginelli, H.E. Roman, R.A. Broglia, F. Alasia, Ab-initio study of the electromagnetic response and polarizability properties of carbon chains.
- [65] L. Henrard, A.A. Lucas, Ph. Lambin, On the 2175 Å absorption band of hollow, onion-like carbon particles, *Astrophys. J.* 406 (1993) 92–96.
- [66] J.B. Kaler, *Cosmic Clouds*, Scientific American Library, New York, 1997.
- [67] A. Bohr, O. Ulfbeck, Primary manifestation of symmetry. Origin of quantal indeterminacy, *Rev. Mod. Phys.* 67 (1995) 1.
- [68] G. Goldstone, Field theories with “superconductor” solutions, *Nuovo Cimento* 19 (1961) 154.
- [69] P. Anderson, *A Career in Theoretical Physics*, World Scientific, Singapore, 1994.
- [70] Y. Nambu, in: T. Eguchi, K. Nishijima (Eds.), *Broken Symmetry*, World Scientific, Singapore, 1995.
- [71] P. Anderson, More is different, *Science* 177 (1972) 393.
- [72] R.A. Broglia, J. Terasaki, N. Giovanardi, The Anderson–Goldstone–Nambu mode in finite and in infinite systems, *Phys. Rep.* 355 (2000) 1–18.
- [73] M.J.G. Veltman, *Scient. Am.*, The Higgs boson, November 1986, p. 88; CERN collider homes in on Higgs boson, *News, Nature* 400 (1999) 601.
- [74] P. Anderson, Use of solid state analogies in elementary particle physics, in: R. Arnowitt, P. Nath (Eds.), *Gauge Theories and Modern Field Theory*, Procs. of a Conference held at Northeastern University, Boston, 26 and 27 September 1975, MIT Press, Cambridge, MA, 1976, p. 311.
- [75] C.M. Lieber, Z. Zhang, Physical properties of metal-doped fullerenes superconductors, *Solid State Phys.* 48 (1994) 349.
- [76] L. Lou, P. Nordlander, R.E. Smalley, Fullerene nanotubes in electric field, *Phys. Rev. B* 52 (1995) 1429–1432.